



SCUOLA INTERNAZIONALE SUPERIORE DI STUDI AVANZATI

SISSA Digital Library

Entanglement negativity in extended systems: a field theoretical approach

Original

Entanglement negativity in extended systems: a field theoretical approach / Calabrese, Pasquale; John, Cardy; Tonni, Erik. - In: JOURNAL OF STATISTICAL MECHANICS: THEORY AND EXPERIMENT. - ISSN 1742-5468. - 2013:2(2013), pp. 1-48. [10.1088/1742-5468/2013/02/P02008]

Availability:

This version is available at: 20.500.11767/17448 since:

Publisher:

Published

DOI:10.1088/1742-5468/2013/02/P02008

Terms of use:

Testo definito dall'ateneo relativo alle clausole di concessione d'uso

Publisher copyright

IOP- Institute of Physics

This version is available for education and non-commercial purposes.

note finali coverpage

(Article begins on next page)

Entanglement negativity in extended systems: A field theoretical approach

Pasquale Calabrese¹, John Cardy², and Erik Tonni³

¹ Dipartimento di Fisica dell'Università di Pisa and INFN, Pisa, Italy.

² Oxford University, Rudolf Peierls Centre for Theoretical Physics, 1 Keble Road, Oxford, OX1 3NP, United Kingdom and All Souls College, Oxford.

³ SISSA and INFN, via Bonomea 265, 34136 Trieste, Italy.

Abstract.

We report on a systematic approach for the calculation of the negativity in the ground state of a one-dimensional quantum field theory. The partial transpose $\rho_A^{T_2}$ of the reduced density matrix of a subsystem $A = A_1 \cup A_2$ is explicitly constructed as an imaginary-time path integral and from this the replicated traces $\text{Tr}(\rho_A^{T_2})^n$ are obtained. The logarithmic negativity $\mathcal{E} = \log ||\rho_A^{T_2}||$ is then the continuation to $n \rightarrow 1$ of the traces of the *even* powers. For pure states, this procedure reproduces the known results. We then apply this method to conformally invariant field theories in several different physical situations for infinite and finite systems and without or with boundaries. In particular, in the case of two adjacent intervals of lengths ℓ_1, ℓ_2 in an infinite system, we derive the result $\mathcal{E} \sim (c/4) \ln(\ell_1 \ell_2 / (\ell_1 + \ell_2))$, where c is the central charge. For the more complicated case of two disjoint intervals, we show that the negativity depends only on the harmonic ratio of the four end-points and so is manifestly scale invariant. We explicitly calculate the scale-invariant functions for the replicated traces in the case of the CFT for the free compactified boson, but we have not so far been able to obtain the $n \rightarrow 1$ continuation for the negativity even in the limit of large compactification radius. We have checked all our findings against exact numerical results for the harmonic chain which is described by a non-compactified free boson.

Contents

1	Introduction	3
1.1	Setup and notations.	4
2	A replica approach for the negativity	5
2.1	Replicas and entanglement entropy.	5
2.2	Replicas and negativity.	6
2.3	Integer powers of the partial transpose and the negativity of a pure state.	6
3	Negativity and Quantum Field Theory	7
3.1	The reduced density matrix and the entanglement entropy in QFT.	8
3.2	The partial transposition and the negativity in QFT.	10
3.3	The case of two adjacent intervals.	11
3.4	The case of a single interval.	11
4	Negativity and conformal invariance: general results	11
4.1	A single interval.	12
4.2	Two adjacent intervals.	13
4.3	Finite systems.	14
5	Negativity for two disjoint intervals in a CFT	14
5.1	The limit of two very close intervals: $y \rightarrow 1$	16
5.2	The limit of two very far intervals: $y \rightarrow 0$	17
5.3	The function $\mathcal{F}_n(x)$ for $0 < x < 1$	17
5.4	The function $\mathcal{G}_n(y)$ and the negativity for a non-compactified boson.	18
5.4.1	The analytic continuation in the limit of close intervals.	19
5.5	The function $\mathcal{G}_n(y)$ and the negativity for the compactified boson.	21
5.5.1	Invariance of $\mathcal{F}_n(x, \bar{x})$ for $x \leftrightarrow 1 - x$ and for $\eta \leftrightarrow 1/\eta$	25
5.5.2	The special case $n = 2$ for the compactified boson.	27
6	Systems with boundaries	28
7	The harmonic chain	29
7.1	Diagonalization and correlation functions of the harmonic chain with periodic boundary conditions.	30
7.2	Diagonalization and correlation functions of the harmonic chain with Dirichlet boundary condition.	31
7.3	The reduced density matrix and its partial transpose.	32
7.4	The negativity for one interval.	33
7.5	The negativity for two adjacent intervals in periodic chains.	35
7.6	The negativity for two disjoint intervals in the periodic chain.	37
7.7	Tripartite chains with Dirichlet boundary in the origin	40
8	Some scaling considerations for massive theories	41
9	Conclusions	42

1. Introduction

The study of the entanglement content of many-body quantum systems has allowed in recent years a deeper understanding of these systems, in particular in connection with criticality and topological order (see [1] for reviews). In the case when a system is in its ground-state (or any given pure state) the entanglement between two complementary parts is measured by the entanglement entropies defined as follows. Let ρ be the density matrix of a system, which we take to be in a pure quantum state $|\Psi\rangle$, so that $\rho = |\Psi\rangle\langle\Psi|$. Let the Hilbert space be written as a direct product $\mathcal{H} = \mathcal{H}_A \otimes \mathcal{H}_B$. A 's reduced density matrix is $\rho_A = \text{Tr}_B \rho$. The entanglement entropy is the corresponding von Neumann entropy

$$S_A = -\text{Tr} \rho_A \ln \rho_A, \quad (1)$$

and analogously for S_B . When ρ corresponds to a pure quantum state $S_A = S_B$. Other standard measures of bipartite entanglement in pure states are the Rényi entropies

$$S_A^{(n)} = \frac{1}{1-n} \ln \text{Tr} \rho_A^n, \quad (2)$$

that also satisfy $S_A^{(n)} = S_B^{(n)}$ whenever ρ corresponds to a pure quantum state. From these definitions $S_A = \lim_{n \rightarrow 1} S_A^{(n)}$. All $S_A^{(n)}$ for any n and for pure states are *entanglement monotonies* [2], i.e. are quantities which do not increase under LOCC (local operation and classical communication), which is a key property of any quantity to be a good measure of entanglement. The knowledge of the Rényi entropies for any n determines also the full spectrum of the reduced density matrix [3].

For a mixed state the entanglement entropies are not longer good measures of entanglement since they mix quantum and classical correlations (e.g. in an high temperature mixed state, S_A gives the extensive result for the thermal entropy that has nothing to do with entanglement). This is also evident from the fact that S_A is no longer equal to S_B . A quantity that is easily constructed from $S_A^{(n)}$ and $S_B^{(n)}$ is the (Rényi) mutual information, defined as

$$I_{A:B}^{(n)} = S_A^{(n)} + S_B^{(n)} - S_{A \cup B}^{(n)}, \quad (3)$$

that by definition is symmetric in A and B . However, $I_{A:B}^{(n)}$ has *not* all the correct properties to be an entanglement measure and indeed it is not an entanglement monotone for any n (for example it has been shown that for most of separable mixed states it is non-zero [4]).

This has also importance for a system in a pure state, but if one is interested into the entanglement between two non-complementary parts A_1 and A_2 . Indeed, generically the union $A_1 \cup A_2$ is in a mixed state with density matrix $\rho_{A_1 \cup A_2} = \text{Tr}_B \rho$ with B the complement of $A_1 \cup A_2$. As a matter of fact, also the converse is true: any mixed state can be obtained by tracing out some degrees of freedom from a properly defined larger system, a procedure called purification (see e.g. [5]).

A proper definition of the bipartite entanglement for a general mixed state (or equivalently the tripartite entanglement in a pure state) has been longly a problem because most of the proposed measures rely on algorithms rather than explicit expressions and are therefore hard to evaluate analytically (see e.g. Refs. [1, 4, 6, 7]). However a *computable measurement of entanglement*, called *negativity*, has been introduced in a seminal work by Vidal and Werner [8]. They also showed how the negativity provides bounds on a few operationally well-defined measures of

entanglement (such as distillable entanglement or teleportation fidelity). The precise meaning of the negativity in quantum information has been indeed established in Ref. [8], but the main reason for its success is a practical one: the negativity is obtained from any mixed state by computing a partial transposition and then diagonalizing a matrix, while we still do not know generically how to compute any other mixed-state entanglement measures.

Following Ref. [8], the negativity is defined as follows. Let us consider a density matrix ρ corresponding to a given mixed or pure state acting on a Hilbert space \mathcal{H} . Let us consider the bipartition $\mathcal{H} = \mathcal{H}_1 \otimes \mathcal{H}_2$ and let us denote by $|e_i^{(1)}\rangle$ and $|e_j^{(2)}\rangle$ two arbitrary bases in the Hilbert spaces of each part. The partial transpose (e.g. with respect to the second space) of ρ is defined as

$$\langle e_i^{(1)} e_j^{(2)} | \rho^{T_2} | e_k^{(1)} e_l^{(2)} \rangle = \langle e_i^{(1)} e_l^{(2)} | \rho | e_k^{(1)} e_j^{(2)} \rangle, \quad (4)$$

and then the *logarithmic* negativity as

$$\mathcal{E} \equiv \ln \|\rho^{T_2}\| = \ln \text{Tr} |\rho^{T_2}|, \quad (5)$$

where the trace norm $\|\rho^{T_2}\|$ is the sum of the absolute values of the eigenvalues λ_i of ρ^{T_2} . In Ref. [8] another measure, termed simply negativity, has been also introduced

$$\mathcal{N} \equiv \frac{\|\rho^{T_2}\| - 1}{2}, \quad (6)$$

which is trivially related to \mathcal{E} as $\mathcal{N} = (e^{\mathcal{E}} - 1)/2$. However, \mathcal{E} is additive, while \mathcal{N} is not and for this reason we will concentrate in the following on \mathcal{E} from which \mathcal{N} can be trivially derived. When the two parts are two microscopic degrees of freedom (e.g. spins), the negativity is equivalent to other commonly used entanglement estimators such as the concurrence [1, 9]. However the definition of the negativity is more appealing because it is basis independent and so calculable by quantum field theory (QFT) which naturally unveils universal features, in particular close to a quantum critical point. For 1D critical theories, that at low energy are also Lorentz invariant, the powerful tools of conformal field theory (CFT) can be applied.

The fact that the negativity is computable made it a remarkable tool to study the tripartite entanglement content of many body quantum systems both in their ground-state [10, 11, 12, 13, 14, 15] or out of equilibrium [16, 17]. Some studies for the bipartite entanglement at finite temperature have been presented as well [18, 19, 20]. However, only in a recent short communication [21], we carried out a more systematic and generic approach to negativity based on QFT (and in particular CFT). In the following we give detailed derivations of all results announced in Ref. [21] and report some other new findings.

1.1. Setup and notations.

In this manuscript we only consider the entanglement, measured by the negativity, in the ground state of one-dimensional systems (1D), although some derivations have a more general validity. We focus on the tripartitions depicted in Fig. 1, i.e. the entire system is divided in three parts A_1 , A_2 and B and we consider the entanglement between A_1 and A_2 , whose union is generically denoted with A . As usual, A 's reduced density matrix is $\rho_A = \text{Tr}_B \rho$. In order to lighten the notation, we will denote as ρ_1 and ρ_2 the reduced density matrix corresponding to A_1 and A_2 respectively, i.e.

$$\rho_1 \equiv \rho_{A_1} = \text{Tr}_{A_2}(\rho_A) = \text{Tr}_{B \cup A_2}(\rho), \quad (7)$$

$$\rho_2 \equiv \rho_{A_2} = \text{Tr}_{A_1}(\rho_A) = \text{Tr}_{B \cup A_1}(\rho). \quad (8)$$

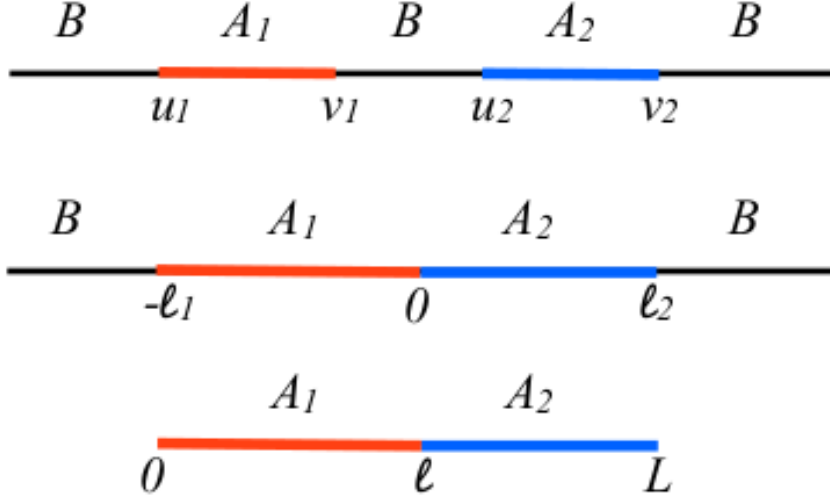


Figure 1. The three main configurations of 1D systems we consider. Top: the entanglement between two disjoint intervals A_1 and A_2 embedded in the ground-state of a larger system formed by the union of A_1 , A_2 and the remainder B . The whole system can be either finite or infinite. Middle: The entanglement between two adjacent intervals in a larger system. Bottom: The entanglement between two adjacent intervals which form the full system ($B \rightarrow \emptyset$). In all cases we denote $A = A_1 \cup A_2$.

Also the partial transpose with respect to A_1 and A_2 degrees of freedom will simply be denoted with the superscripts T_1 and T_2 respectively, i.e.

$$\rho_A^{T_2} \equiv \rho_A^{T_{A_2}}, \quad \text{and} \quad \rho_A^{T_1} \equiv \rho_A^{T_{A_1}}. \quad (9)$$

2. A replica approach for the negativity

2.1. Replicas and entanglement entropy.

One of the most successful approaches to calculate the entanglement entropy for a bipartite system is based on the replica trick [22] which proceeds as follows. One first calculates the traces of integer powers of the reduced density matrix

$$\text{Tr} \rho_2^n = \sum_i \zeta_i^n, \quad (10)$$

where ζ_i are the eigenvalues of the reduced density matrix ρ_2 . Then, if one is able to analytically continue this expression to general complex n , the entanglement entropy is given by

$$S_{A_2} = - \lim_{n \rightarrow 1} \frac{\partial}{\partial n} \text{Tr} \rho_2^n = \lim_{n \rightarrow 1} \frac{1}{1-n} \ln \text{Tr} \rho_2^n. \quad (11)$$

It has been shown [22, 23] that, for integer n , $\text{Tr} \rho_2^n$ is a partition function on a complicated Riemann surface (or equivalently the correlation function of specific *twist fields*, as we shall review later) that is analytically achievable in a quantum field theory. The analytical properties of $\text{Tr} \rho_2^n$ in the complex plane of replicas are also discussed in Refs. [24, 25].

2.2. Replicas and negativity.

A natural way to use a replica trick to compute the negativity would be to relate it to the traces of integer powers of ρ^{T_2} . The trace norm of ρ^{T_2} can be written in terms of its eigenvalues λ_i as

$$\text{Tr}|\rho^{T_2}| = \sum_i |\lambda_i| = \sum_{\lambda_i > 0} |\lambda_i| + \sum_{\lambda_i < 0} |\lambda_i| = 1 + 2 \sum_{\lambda_i < 0} |\lambda_i|, \quad (12)$$

where in the last equality we used the normalization $\sum_i \lambda_i = 1$. This expression makes evident that the negativity measures “how much” the eigenvalues of the partial transpose of the density matrix are negative, a properties which is the reason of the name negativity.

The traces $\text{Tr}(\rho^{T_2})^n$ of integer powers of ρ^{T_2} have a difference dependence on $|\lambda_i|$ depending on the parity of n . In the following we will always indicate an even $n = 2m$ as n_e while an odd one $n = 2m + 1$ with n_o . It is understood that n_e and n_o refer always to the same thing, it is just the functional dependence of the traces which is different. In fact, for n even and odd, the traces of integer powers of ρ^{T_2} are

$$\text{Tr}(\rho^{T_2})^{n_e} = \sum_i \lambda_i^{n_e} = \sum_{\lambda_i > 0} |\lambda_i|^{n_e} + \sum_{\lambda_i < 0} |\lambda_i|^{n_e}, \quad (13)$$

$$\text{Tr}(\rho^{T_2})^{n_o} = \sum_i \lambda_i^{n_o} = \sum_{\lambda_i > 0} |\lambda_i|^{n_o} - \sum_{\lambda_i < 0} |\lambda_i|^{n_o}. \quad (14)$$

If now we just set $n_e = 1$ in Eq. (13) we formally obtain $\text{Tr}|\rho^{T_2}|$ in which we are interested. Oppositely, setting $n_o = 1$ in Eq. (14) gives the normalization $\text{Tr}\rho^{T_2} = 1$. This means that the analytic continuations from even and odd n are different and the trace norm in which we are interested is obtained by considering the analytic continuation of the even sequence at $n_e \rightarrow 1$, i.e.

$$\mathcal{E} = \lim_{n_e \rightarrow 1} \ln \text{Tr}(\rho^{T_2})^{n_e}. \quad (15)$$

We should also mention that being $(\rho^{T_2})^T = \rho^{T_1}$, it trivially holds $\text{Tr}(\rho^{T_2})^n = \text{Tr}(\rho^{T_1})^n$ for any n , even not integer.

At first, this approach can seem rather unnatural because what we are doing is basically propose to calculate a quantity for even numbers and at the end set this even number to 1 which is instead odd. However, similar replica calculations have been already successfully applied to other different physical problems [26, 27], showing the reasonableness of the approach.

2.3. Integer powers of the partial transpose and the negativity of a pure state.

As a first example and check of the replica trick, we consider the case of a bipartition of the Hilbert spaces $\mathcal{H} = \mathcal{H}_1 \otimes \mathcal{H}_2$ of a pure state $|\Psi\rangle$ with $\rho = |\Psi\rangle\langle\Psi|$ for which the negativity is known [8]. The Schmidt decomposition, in terms of two bases $|e_k^{(1)}\rangle$ and $|e_j^{(2)}\rangle$ in the Hilbert spaces \mathcal{H}_1 and \mathcal{H}_2 respectively, gives

$$|\Psi\rangle = \sum_j c_j |e_j^{(1)} e_j^{(2)}\rangle \quad (16)$$

where the coefficient c_j can be chosen such that $c_j \in [0, 1]$. We also have

$$\rho = \sum_{j,k} c_j c_k |e_j^{(1)} e_j^{(2)}\rangle \langle e_k^{(1)} e_k^{(2)}|, \quad \rho_2 = \text{Tr}_1(\rho) = \sum_j c_k^2 |e_k^{(2)}\rangle \langle e_k^{(2)}|, \quad (17)$$

where ρ_2 is the reduced density matrix on \mathcal{H}_2 .

The partial transpose of the density matrix is then

$$\rho^{T_2} = \sum_{j,k} c_j c_k |e_j^{(1)} e_k^{(2)}\rangle \langle e_k^{(1)} e_j^{(2)}|, \quad (18)$$

whose n -th power reads

$$\begin{aligned} (\rho^{T_2})^n &= \sum_{\substack{j_1, \dots, j_n \\ k_1, \dots, k_n}} c_{j_1} c_{k_1} c_{j_2} c_{k_2} \dots c_{j_n} c_{k_n} \\ &\quad \times |e_{k_1}^{(2)} e_{j_1}^{(1)}\rangle \langle e_{j_1}^{(2)} e_{k_1}^{(1)}| |e_{k_2}^{(2)} e_{j_2}^{(1)}\rangle \langle e_{j_2}^{(2)} e_{k_2}^{(1)}| \dots |e_{k_n}^{(2)} e_{j_n}^{(1)}\rangle \langle e_{j_n}^{(2)} e_{k_n}^{(1)}| = \\ &= \sum_{\substack{j_1, \dots, j_n \\ k_1, \dots, k_n}} c_{j_1} c_{k_1} c_{j_2} c_{k_2} \dots c_{j_n} c_{k_n} \\ &\quad \times |e_{k_1}^{(2)} e_{j_1}^{(1)}\rangle \delta_{j_1, k_2} \delta_{k_1, j_2} \delta_{j_2, k_3} \delta_{k_2, j_3} \dots \delta_{j_{n-1}, k_n} \delta_{k_{n-1}, j_n} \langle e_{j_n}^{(2)} e_{k_n}^{(1)}|. \end{aligned} \quad (19)$$

The sequence of deltas gives a result which depends on the parity of n

$$(\rho^{T_2})^n = \begin{cases} \sum_{j_1, k_1} c_{j_1}^{n_o} c_{k_1}^{n_o} |e_{k_1}^{(2)} e_{j_1}^{(1)}\rangle \langle e_{j_1}^{(2)} e_{k_1}^{(1)}|, & n = n_o \text{ odd}, \\ \sum_{j_1, k_1} c_{j_1}^{n_e} c_{k_1}^{n_e} |e_{k_1}^{(2)} e_{j_1}^{(1)}\rangle \langle e_{k_1}^{(2)} e_{j_1}^{(1)}|, & n = n_e \text{ even}, \end{cases} \quad (20)$$

from which

$$\text{Tr}(\rho^{T_2})^n = \begin{cases} \sum_r c_r^{2n_o} = \text{Tr} \rho_2^{n_o}, & n = n_o \text{ odd}, \\ \left[\sum_r c_r^{n_e} \right]^2 = (\text{Tr} \rho_2^{n_e/2})^2, & n = n_e \text{ even}. \end{cases} \quad (21)$$

Notice in particular that

$$\text{Tr}(\rho^{T_2})^2 = \text{Tr}(\rho^{T_2}) = 1. \quad (22)$$

Taking the limit $n_e \rightarrow 1$, we recover the result [8] that for a pure state the logarithmic negativity is the Rényi entropy of order $1/2$ (cf. Eq. (2) with $n = 1/2$)

$$\mathcal{E} = S_{A_2}^{(1/2)} = 2 \ln \text{Tr} \rho_2^{1/2}. \quad (23)$$

Taking instead the limit $n_o \rightarrow 1$, we recover the normalization $\text{Tr}(\rho^{T_2}) = \text{Tr} \rho_2 = 1$.

3. Negativity and Quantum Field Theory

In this section we show how to compute for a generic tripartition of a 1D quantum field theory the integer traces of the partial transpose of the reduced density matrix and from these, via the replica trick, the logarithmic negativity. For concreteness we will only consider the *tripartition* of a 1D system depicted in Fig. 1 with A composed of two parts $A = A_1 \cup A_2 = [u_1, v_1] \cup [u_2, v_2]$ and B the remainder, but most of the following ideas apply to more general cases (e.g. A_1 and A_2 made each of several disjoint intervals). In order to introduce the general formalism for the negativity, we first review in the next subsection the path integral approach to the entanglement entropy [22, 23] and the use of the twist fields [22, 24].

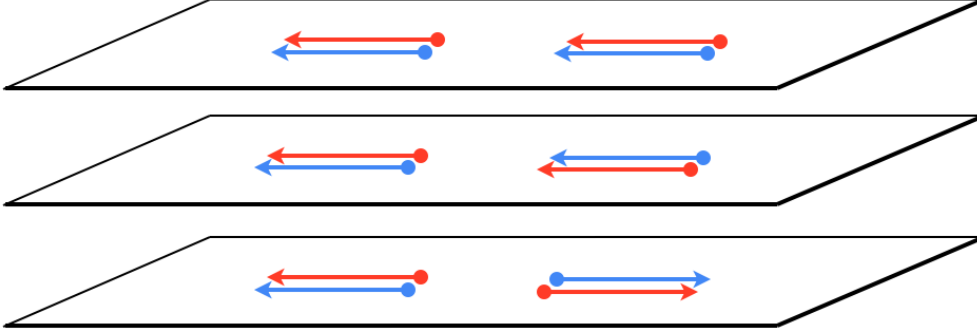


Figure 2. Top: The reduced density matrix ρ_A of two disjoint intervals. Middle: Partial transpose with respect to the second interval $\rho_A^{T_2}$. Bottom: Reversed partial transpose $\rho_A^{C_2} = C \rho_A^{T_2} C$, where C reverses the order of the row and column indices.

3.1. The reduced density matrix and the entanglement entropy in QFT.

The density matrix ρ in a thermal state at temperature $T = 1/\beta$ may be written as a path integral in the imaginary time interval $(0, \beta)$

$$\rho(\{\phi_x\}|\{\phi'_{x'}\}) = Z^{-1} \int [d\phi(y, \tau)] \prod_x \delta(\phi(y, 0) - \phi'_{x'}) \prod_x \delta(\phi(y, \beta) - \phi_x) e^{-S_E}, \quad (24)$$

where $Z = \text{Tr} e^{-H/T}$ is the partition function and S_E is the euclidean action. Here the rows and columns of the density matrix are labelled by the values of the fields $\{\phi_x\}$ at $\tau = 0, \beta$. The normalization factor Z ensures $\text{Tr} \rho = 1$, and is found by setting $\{\phi_x\} = \{\phi'_{x'}\}$ and integrating over these variables. In the path integral, this has the effect of sewing together the two edges to form a cylinder of circumference β .

Now let us consider the subsystem A in Fig. 1 composed of two parts $A = A_1 \cup A_2 = [u_1, v_1] \cup [u_2, v_2]$. The reduced density matrix ρ_A is obtained from (24) by sewing together only those points x which are not in A . This has the effect of leaving two open cuts, one for each interval (u_j, v_j) , along the line $\tau = 0$. In the limit of zero temperature, i.e. for the ground-state of the QFT, the cylinder becomes a plane as in Fig. 2 (top) where the two open cuts correspond to the rows and columns of ρ_A and the orientation of the arrows gives the ordering of the row/column indices, e.g. increasing along the directions of the arrows.

We may then compute $\text{Tr} \rho_A^n$, for any positive integer n , by making n copies of the above, labelled by an integer j with $1 \leq j \leq n$, and sewing them together cyclically along the the cuts so that $\phi_j(x, \tau = 0^-) = \phi_{j+1}(x, \tau = 0^+)$ and $\phi_n(x, \tau = 0^-) = \phi_1(x, \tau = 0^+)$ for all $x \in A$. This defines the n -sheeted Riemann surface \mathcal{R}_n depicted for $n = 3$ in Fig. 3. Denoting with $Z_{\mathcal{R}_n}$ the partition function on this surface we have

$$\text{Tr} \rho_A^n = \frac{Z_{\mathcal{R}_n}}{Z^n}. \quad (25)$$

This expression gives the Rényi entropies in Eq. (2) for integer n and through the analytic continuation the entanglement entropy in Eq. (1).

As a consequence of its locality, the partition function can be expressed as an object calculated on the complex plane \mathbb{C} , where the structure of the Riemann surface is implemented through appropriate boundary conditions around the points with non-zero curvature, i.e. the partition function in a theory defined on the complex plane

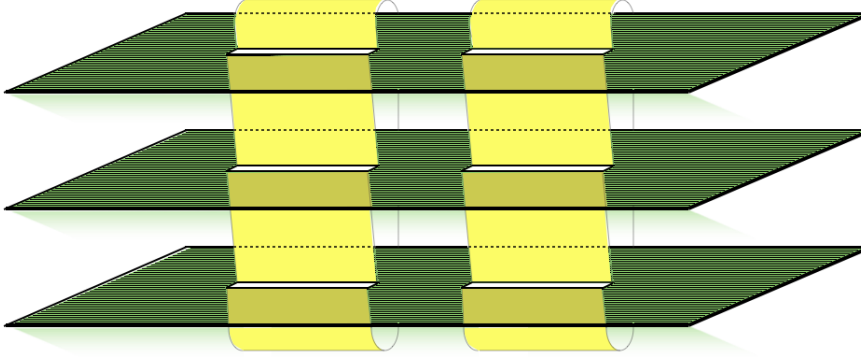


Figure 3. The path integral representation of $\text{Tr}\rho_A^n$ gives a n -sheeted Riemann surface \mathcal{R}_n depicted here for $n = 3$ and $A = [u_1, v_1] \cup [u_2, v_2]$.

$z = x + i\tau$ should be written in terms of certain “fields” at $z = v_j$ and $z = u_j$. The partition function (here $\mathcal{L}[\phi](z, \bar{z})$ is the lagrangian density)

$$Z_{\mathcal{R}_n} = \int [d\phi]_{\mathcal{R}_n} \exp \left[- \int_{\mathcal{R}_n} dz d\bar{z} \mathcal{L}[\phi](z, \bar{z}) \right], \quad (26)$$

essentially defines these fields. Following Ref. [24], it is useful to move the topology of the world-sheet (i.e. the space where the coordinates x, τ lie) \mathcal{R}_n to the target space (i.e. the space where the fields lie). To this aim, let us consider a model formed by n independent copies of the original model. The partition function (26) can be re-written as the path integral on the complex plane

$$Z_{\mathcal{R}_n} = \int_{\mathcal{C}_{u_j, v_j}} [d\phi_1 \cdots d\phi_n]_{\mathbb{C}} \exp \left[- \int_{\mathbb{C}} dz d\bar{z} (\mathcal{L}[\phi_1](z, \bar{z}) + \dots + \mathcal{L}[\phi_n](z, \bar{z})) \right], \quad (27)$$

where with $\int_{\mathcal{C}_{u_j, v_j}}$ we indicated the *restricted* path integral with conditions

$$\mathcal{C}_{u_j, v_j} : \quad \phi_i(x, 0^+) = \phi_{i+1}(x, 0^-), \quad x \in [u_1, v_1] \cup [u_2, v_2], \quad i = 1, \dots, n, \quad (28)$$

where $n + i \equiv i$. The lagrangian density of the multi-copy model is

$$\mathcal{L}^{(n)}[\phi_1, \dots, \phi_n](x, \tau) = \mathcal{L}[\phi_1](x, \tau) + \dots + \mathcal{L}[\phi_n](x, \tau), \quad (29)$$

so that the energy density is the sum of the energy densities of the n individual copies. Hence the expression (27) indeed defines local fields at $(u_j, 0)$ and $(v_j, 0)$ in the multi-copy model [24].

The local fields defined in (27) are examples of *twist fields*. Twist fields exist in a QFT whenever there is a global internal symmetry σ , i.e. $\int dx d\tau \mathcal{L}[\sigma\phi](x, \tau) = \int dx d\tau \mathcal{L}[\phi](x, \tau)$. The twist fields defined by (27), called *branch-point twist fields* [24], are associated to the two opposite cyclic permutation symmetries $i \mapsto i + 1$ and $i + 1 \mapsto i$. We can denote them simply by \mathcal{T}_n and $\bar{\mathcal{T}}_n$

$$\mathcal{T}_n \equiv \mathcal{T}_{\sigma}, \quad \sigma : i \mapsto i + 1 \bmod n, \quad (30)$$

$$\bar{\mathcal{T}}_n \equiv \mathcal{T}_{\sigma^{-1}}, \quad \sigma^{-1} : i + 1 \mapsto i \bmod n. \quad (31)$$

$\bar{\mathcal{T}}_n$ can be identified with \mathcal{T}_{-n} and $\mathcal{T}_n^n = \bar{\mathcal{T}}_n^n = 1$. Thus, for the n -sheeted Riemann surface along the set A made of the two disjoint intervals $[u_1, v_1] \cup [u_2, v_2]$, we have

$$\text{Tr}\rho_A^n = \langle \mathcal{T}_n(u_1) \bar{\mathcal{T}}_n(v_1) \mathcal{T}_n(u_2) \bar{\mathcal{T}}_n(v_2) \rangle_{\mathbb{C}}. \quad (32)$$

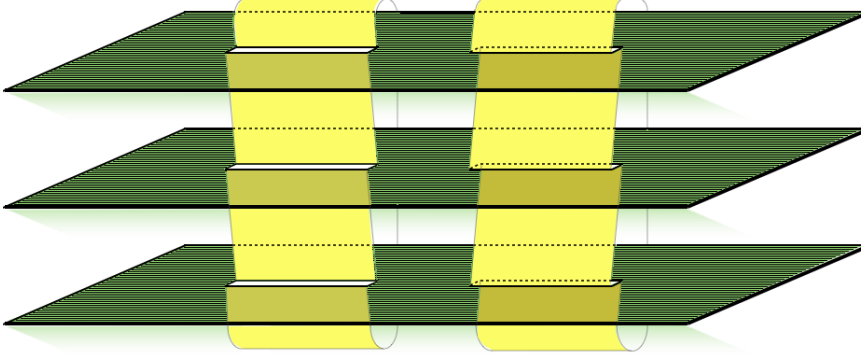


Figure 4. Path integral representation of $\text{Tr}(\rho_A^{T_2})^n = \text{Tr}(\rho_A^{C_2})^n$ for $n = 3$.

In the following the subscript \mathbb{C} will be understood in the expectation values, if not differently stated.

3.2. The partial transposition and the negativity in QFT.

The partial transposition of the reduced density matrix ρ_A with respect to the second interval A_2 corresponds to the exchange of row and column indices in A_2 . In the path integral representation, this is equivalent to interchange the upper and lower edges of the second cut in ρ_A as depicted in the middle of Fig. 2. If we join n copies of $\rho_A^{T_2}$ cyclically, we have an n -sheeted Riemann surface where row and column indices are reversed compared to those of a correlation function of four twist fields, as it should be clear from the middle of Fig. 2. This problem can be however solved very easily by reversing the order of the column and row indices in A_2 as in the bottom of Fig. 2, to obtain the *reversed partial transpose* $\rho_A^{C_2}$. This is related to the partial transpose as $\rho_A^{C_2} = C \rho_A^{T_2} C$, where C reverses the order of indices either on the lower or on the upper cut and satisfies $C^2 = 1$. Clearly $\text{Tr}(\rho_A^{T_2})^n = \text{Tr}(\rho_A^{C_2})^n$ and so $\text{Tr}(\rho_A^{T_2})^n$ is the partition function on the n -sheeted surface obtained by joining cyclically n of the above $\rho_A^{C_2}$ as in Fig. 4. In this case, the order of the row and column indices is the right one to identify this partition function with the four-point function of the twist fields

$$\text{Tr}(\rho_A^{T_2})^n = \text{Tr}(\rho_A^{C_2})^n = \langle \mathcal{T}_n(u_1) \bar{\mathcal{T}}_n(v_1) \bar{\mathcal{T}}_n(u_2) \mathcal{T}_n(v_2) \rangle, \quad (33)$$

i.e. the partial transposition has the net effect to exchange two twist operators compared to Eq. (32). We notice that we could easily have worked out $\text{Tr}(\rho_A^{T_2})^n$ without introducing the reverse partial transpose. However this is a very useful technical concept because it allows to identify $\text{Tr}(\rho_A^{T_2})^n$ with the correlation function of already known and studied twist fields, without the need of introducing new fields.

For $n = 2$, $\mathcal{T}_2 = \bar{\mathcal{T}}_2$ and so

$$\text{Tr} \rho_A^2 = \text{Tr}(\rho_A^{T_2})^2, \quad (34)$$

which also straightforwardly follows from the properties of the trace and so it is true for any matrix ρ replacing ρ_A above.

To replace $\rho_A^{T_2}$ with $\rho_A^{C_2}$ it has been fundamental to consider integer cyclical traces. The operator C enters in quantities like $\text{Tr}(\rho_A \rho_A^{T_2})$ which is in fact the partition

function on a non-orientable surface with the topology of a Klein bottle. This can also be computed using CFT methods [28].

3.3. The case of two adjacent intervals.

Eq. (33) is of general validity, but it has interesting simple and general consequences when specialized to the case of two adjacent intervals. This can be obtained by letting $v_1 \rightarrow u_2$ so that

$$\text{Tr}(\rho_A^{T_2})^n = \langle \mathcal{T}_n(u_1) \overline{\mathcal{T}}_n(u_2) \mathcal{T}_n(v_2) \rangle. \quad (35)$$

For arbitrary n , this expression cannot be evaluated in general, but two cases are easily worked out.

For $n = 2$, we have $\mathcal{T}_2^2 = 1$ and so

$$\text{Tr}(\rho_A^{T_2})^2 = \langle \mathcal{T}_2(u_1) \mathcal{T}_2(v_2) \rangle = \text{Tr} \rho_{A_1 \cup A_2}^2. \quad (36)$$

This relation has been derived here from QFT methods and it would be interesting to know its general validity.

For $n = 3$, we have $\overline{\mathcal{T}}_3^2 = \mathcal{T}_3$ and so

$$\text{Tr}(\rho_A^{T_2})^3 = \langle \mathcal{T}_3(u_1) \mathcal{T}_3(u_2) \mathcal{T}_3(v_2) \rangle. \quad (37)$$

3.4. The case of a single interval.

We now specialize to a pure state by letting $B \rightarrow \emptyset$ for which $\text{Tr}(\rho_A^{T_2})^n$ can be worked out in full generality considering $u_2 \rightarrow v_1$ and $v_2 \rightarrow u_1$

$$\text{Tr}(\rho_A^{T_2})^n = \langle \mathcal{T}_n^2(u_2) \overline{\mathcal{T}}_n^2(v_2) \rangle. \quad (38)$$

This expression depends on the parity of n because \mathcal{T}_n^2 connects the j -th sheet with the $(j+2)$ -th one. For $n = n_e$ even, the n_e -sheeted Riemann surface decouples in two independent $(n_e/2)$ -sheeted surfaces characterized by the parity of the sheets. Conversely for $n = n_o$ odd, the surface remains a n_o -sheeted Riemann surface (a part from a shuffling of the sheets). This is pictorially shown in Fig. 5. Thus we have

$$\begin{aligned} \text{Tr}(\rho_A^{T_2})^{n_e} &= (\langle \mathcal{T}_{n_e/2}(u_2) \overline{\mathcal{T}}_{n_e/2}(v_2) \rangle)^2 = (\text{Tr} \rho_{A_2}^{n_e/2})^2, \\ \text{Tr}(\rho_A^{T_2})^{n_o} &= \langle \mathcal{T}_{n_o}(u_2) \overline{\mathcal{T}}_{n_o}(v_2) \rangle = \text{Tr} \rho_{A_2}^{n_o}, \end{aligned} \quad (39)$$

which are the results for pure states in Eq. (21), recovered here purely from QFT and showing in a first simple example the effect of the parity of n on the Riemann surfaces.

4. Negativity and conformal invariance: general results

In this section we explicitly calculate the negativity for those situations in CFT where $\text{Tr}(\rho_A^{T_2})^n$ can be fixed by global conformal invariance and so does not depend on the operator content of the theory, but only on the central charge.

Before embarking in the full negativity calculation, we should recall that $\text{Tr} \rho_A^n$, for the case of a single interval $A = [u_1, v_1]$, has been obtained by uniformizing the n -sheeted Riemann surface to the complex plane [22]. This shows that the twist fields transform like primary operators of dimension [22]

$$\Delta_{\mathcal{T}_n} = \Delta_{\overline{\mathcal{T}}_n} = \frac{c}{12} \left(n - \frac{1}{n} \right), \quad (40)$$

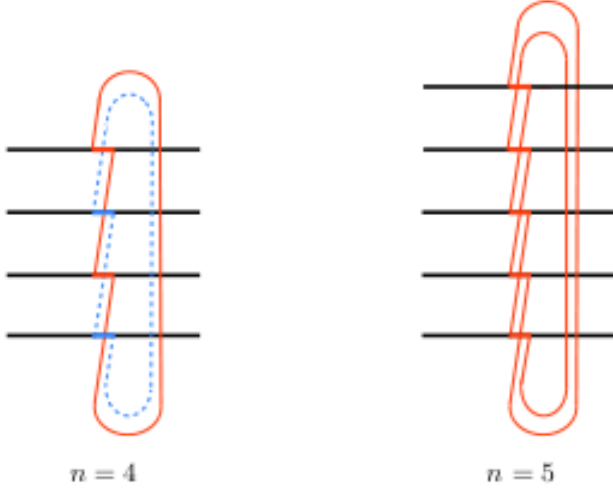


Figure 5. Cut of the Riemann surface defined by $\langle \mathcal{T}_n^2(u_2) \bar{\mathcal{T}}_n^2(v_2) \rangle$. Left: A typical example for n even ($n = 4$ in the figure) showing how the surface decouples in two independent parts, each with half of the sheets. Right: A typical example for n odd ($n = 5$ in the figure) showing that the net effect is just a reshuffling of the sheet numeration going from $(1, 2, 3, 4, 5)$ to $(1, 3, 5, 2, 4)$.

where c is the central charge. This implies ($\ell = |u_1 - v_1|$) [29, 30, 22]

$$\text{Tr} \rho_A^n = c_n \left(\frac{\ell}{a} \right)^{-c/6(n-1/n)} \Rightarrow S_A = \frac{c}{3} \ln \frac{\ell}{a} + c'_1, \quad (41)$$

where a is an UV cutoff (e.g. the lattice spacing) and c_n a non-universal constant, with $c_1 = 1$. After the normalization of the two-point function of twist fields on the plane is fixed by the constants c_n , the normalizations of two-point functions in arbitrary geometry and all other multi-point correlation functions of the twist fields are fixed and universal. Furthermore, although non-universal, the constants c_n satisfy some universal relations (see e.g. [31]).

4.1. A single interval.

Even for conformal invariant theories it is useful to specialize first to the very simple case of a reduced density matrix corresponding to a pure system, which is obtained by letting $B \rightarrow \emptyset$. Thus, when A_2 is embedded in an infinite system, from Eqs. (39) and (41) we have (setting $\ell = u_2 - v_2$)

$$\text{Tr}(\rho_A^{T_2})^{n_e} = (\langle \mathcal{T}_{n_e/2}(u_2) \bar{\mathcal{T}}_{n_e/2}(v_2) \rangle)^2 = (\text{Tr} \rho_{A_2}^{n_e/2})^2 = c_{n_e/2}^2 \left(\frac{\ell}{a} \right)^{-c/3(n_e/2-2/n_e)}, \quad (42)$$

and

$$\text{Tr}(\rho_A^{T_2})^{n_o} = \langle \mathcal{T}_{n_o}(u_2) \bar{\mathcal{T}}_{n_o}(v_2) \rangle = \text{Tr} \rho_{A_2}^{n_o} = c_{n_o} \left(\frac{\ell}{a} \right)^{-c/6(n_o-1/n_o)}. \quad (43)$$

In spite of the simplicity of the above calculation, it shows one important point of the CFT analysis: for $n = n_e$ even, $\mathcal{T}_{n_e}^2$ and $\bar{\mathcal{T}}_{n_e}^2$ have dimensions

$$\Delta_{\mathcal{T}_{n_e}^2} = \Delta_{\bar{\mathcal{T}}_{n_e}^2} = \frac{c}{6} \left(\frac{n_e}{2} - \frac{2}{n_e} \right), \quad (44)$$

while for $n = n_o$ odd, $\mathcal{T}_{n_o}^2$ and $\bar{\mathcal{T}}_{n_o}^2$ have dimensions

$$\Delta_{\mathcal{T}_{n_o}^2} = \Delta_{\bar{\mathcal{T}}_{n_o}^2} = \frac{c}{12} \left(n_o - \frac{1}{n_o} \right), \quad (45)$$

the same as \mathcal{T}_{n_o} . Thus, performing the analytic continuation from the even branch, we finally have

$$\|\rho_A^{T_2}\| = \lim_{n_e \rightarrow 1} \text{Tr}(\rho_A^{T_2})^{n_e} = c_{1/2}^2 \left(\frac{\ell}{a} \right)^{c/2} \Rightarrow \mathcal{E} = \frac{c}{2} \ln \frac{\ell}{a} + 2 \ln c_{1/2}, \quad (46)$$

which, again, just tells us that for pure states the logarithmic negativity equals the Rényi entropy of order $1/2$. Continuing instead to $n_o \rightarrow 1$ from the odd branch we obtain the normalization $\text{Tr} \rho_A^{T_2} = 1$.

Notice that although the various constants c_{n_o, n_e} are non-universal, they are the same appearing in the entanglement entropies.

4.2. Two adjacent intervals.

Let us now consider the non-trivial configuration in which two intervals A_1 and A_2 of length ℓ_1 and ℓ_2 share a common boundary (let us say at the origin) as graphically depicted in Fig. 1. This can be obtained by letting $v_1 \rightarrow u_2 = 0$ in Eq. (33) and it is then described by the 3-point function (we set $u_1 = -\ell_1$ and $v_2 = \ell_2$)

$$\text{Tr}(\rho_A^{T_2})^n = \langle \mathcal{T}_n(-\ell_1) \bar{\mathcal{T}}_n^2(0) \mathcal{T}_n(\ell_2) \rangle, \quad (47)$$

whose form is determined by conformal symmetry [63]

$$\langle \mathcal{T}_n(-\ell_1) \bar{\mathcal{T}}_n^2(0) \mathcal{T}_n(\ell_2) \rangle = c_n^2 \frac{C_{\mathcal{T}_n \bar{\mathcal{T}}_n^2 \mathcal{T}_n}}{(\ell_1 \ell_2)^{\Delta_{\mathcal{T}_n^2}} (\ell_1 + \ell_2)^{2\Delta_{\mathcal{T}_n} - \Delta_{\mathcal{T}_n^2}}}, \quad (48)$$

which has been normalized in such a way that the structure constant $C_{\mathcal{T}_n \bar{\mathcal{T}}_n^2 \mathcal{T}_n}$ is universal (with all the lengths ℓ_j measured in units of the UV cutoff a) and can be determined by considering the proper limit of the four-point function, as it will be done in next section.

For $n = n_e$ even, using the dimensions of the twist operators calculated above, we find

$$\text{Tr}(\rho_A^{T_2})^{n_e} \propto (\ell_1 \ell_2)^{-c/6(n_e/2 - 2/n_e)} (\ell_1 + \ell_2)^{-c/6(n_e/2 + 1/n_e)}, \quad (49)$$

that in the limit $n_e \rightarrow 1$ gives

$$\|\rho_A^{T_2}\| \propto \left(\frac{\ell_1 \ell_2}{\ell_1 + \ell_2} \right)^{c/4} \Rightarrow \mathcal{E} = \frac{c}{4} \ln \frac{\ell_1 \ell_2}{\ell_1 + \ell_2} + \text{cnst.} \quad (50)$$

For $n = n_o$ odd

$$\text{Tr}(\rho_A^{T_2})^{n_o} \propto (\ell_1 \ell_2 (\ell_1 + \ell_2))^{-\frac{c}{12}(n_o - 1/n_o)}, \quad (51)$$

that for $n_o \rightarrow 1$ gives again $\text{Tr} \rho_A^{T_2} = 1$ as it should.

Notice that for $n = 2$, Eq. (49) is

$$\text{Tr}(\rho_A^{T_2})^2 = c_2^2 C_{\mathcal{T}_2 \bar{\mathcal{T}}_2^2 \mathcal{T}_2} (\ell_1 + \ell_2)^{-c/4}, \quad (52)$$

which equals $\text{Tr} \rho_{A_1 \cup A_2}^2$, as predicted by Eq. (36), if $C_{\mathcal{T}_2 \bar{\mathcal{T}}_2^2 \mathcal{T}_2} = c_2^{-1}$.

4.3. Finite systems.

All the previous results may be generalized to the case of a finite system of length L with periodic boundary conditions by using a conformal mapping from the cylinder to the plane. The net effect of the mapping is to replace each length ℓ_i with the chord length $(L/\pi) \sin(\pi \ell_i/L)$ in all above formulas.

Thus for the case of a pure state in a finite system the generalization of Eqs. (42) and (43) are

$$\text{Tr}(\rho_A^{T_2})^{n_e} = c_{n_e/2}^2 \left(\frac{L}{\pi a} \sin \frac{\pi \ell}{L} \right)^{-c/3(n_e/2-2/n_e)}, \quad (53)$$

$$\text{Tr}(\rho_A^{T_2})^{n_o} = c_{n_o} \left(\frac{L}{\pi a} \sin \frac{\pi \ell}{L} \right)^{-c/6(n_o-1/n_o)}, \quad (54)$$

$$\mathcal{E} = \frac{c}{2} \ln \left(\frac{L}{\pi a} \sin \frac{\pi \ell}{L} \right) + 2 \ln c_{1/2}. \quad (55)$$

For the case of two adjacent intervals the finite system generalizations of Eqs. (49) and (51) are

$$\begin{aligned} \text{Tr}(\rho_A^{T_2})^{n_e} &\propto \left[\frac{L^2}{\pi^2} \sin \left(\frac{\pi \ell_1}{L} \right) \sin \left(\frac{\pi \ell_2}{L} \right) \right]^{-c/6(n_e/2-2/n_e)} \left[\frac{L}{\pi} \sin \frac{\pi(\ell_1 + \ell_2)}{L} \right]^{-\frac{c}{6}(\frac{n_e}{2} + \frac{1}{n_e})}, \\ \text{Tr}(\rho_A^{T_2})^{n_o} &\propto \left[\frac{L^3}{\pi^3} \sin \left(\frac{\pi \ell_1}{L} \right) \sin \left(\frac{\pi \ell_2}{L} \right) \sin \frac{\pi(\ell_1 + \ell_2)}{L} \right]^{-c/12(n_o-1/n_o)}, \end{aligned} \quad (56)$$

leading to the logarithmic negativity

$$\mathcal{E} = \frac{c}{4} \ln \left[\frac{L \sin \left(\frac{\pi \ell_1}{L} \right) \sin \left(\frac{\pi \ell_2}{L} \right)}{\pi \sin \frac{\pi(\ell_1 + \ell_2)}{L}} \right] + \text{cnst.} \quad (57)$$

5. Negativity for two disjoint intervals in a CFT

For the more difficult situation of two disjoint intervals reported in Fig. 1, the entanglement entropies depend on the full operator content of the CFT and this makes much more complicated also the calculation of the negativity.

Global conformal invariance fixes the form of the four-point correlation of twist fields

$$\langle \mathcal{T}_n(z_1) \overline{\mathcal{T}}_n(z_2) \mathcal{T}_n(z_3) \overline{\mathcal{T}}_n(z_4) \rangle = c_n^2 \left| \frac{z_{31} z_{42}}{z_{21} z_{43} z_{41} z_{32}} \right|^{c/6(n-1/n)} \mathcal{F}_n(x, \bar{x}), \quad (58)$$

with x the four point ratio

$$x = \frac{z_{21} z_{43}}{z_{31} z_{42}}, \quad (59)$$

and $z_{ij} = z_i - z_j$. Notice that $z_{31} z_{42}/(z_{21} z_{43} z_{41} z_{32}) = 1/(z_{21} z_{43}(1-x))$. This is normalized in such a way that $\mathcal{F}_n(0, 0) = 1$ (for $x \rightarrow 0$, the four-point function is the product of the two two-point functions normalized with c_n). The function $\mathcal{F}_n(x, \bar{x})$ depends explicitly on the full operator content of the theory and must be calculated case by case. Notice that with $\mathcal{F}_1(x, \bar{x}) = 1$ as a consequence of $\text{Tr} \rho_A = 1$.

Now, according to Eq. (32), $\text{Tr} \rho_A^n$ corresponds in Eq. (58) to the choice

$$z_1 = u_1, \quad z_2 = v_1, \quad z_3 = u_2, \quad z_4 = v_2, \quad (60)$$

and so

$$\text{Tr} \rho_A^n = c_n^2 \left(\frac{(u_2 - u_1)(v_2 - v_1)}{(v_1 - u_1)(v_2 - u_2)(v_2 - u_1)(u_2 - v_1)} \right)^{c/6(n-1/n)} \mathcal{F}_n(x), \quad (61)$$

where, since for real u_j and v_j the ratio x is real, we dropped the dependence on $\bar{x} = x$. Explicitly, in this case x is

$$x = \frac{(v_1 - u_1)(v_2 - u_2)}{(u_2 - u_1)(v_2 - v_1)}, \quad (62)$$

that for the order $u_1 < v_1 < u_2 < v_2$ satisfies $0 < x < 1$.

Even $\text{Tr}(\rho_A^{T_2})^n$ is a four-point function of twist fields according to Eq. (33), but it corresponds in Eq. (58) to the choice

$$z_1 = u_1, \quad z_2 = v_1, \quad z_3 = v_2, \quad z_4 = u_2, \quad (63)$$

i.e. to the exchange $z_3 \leftrightarrow z_4$ compared to $\text{Tr} \rho_A^n$. Thus we can write

$$\text{Tr}(\rho_A^{T_2})^n = c_n^2 \left(\frac{(v_2 - u_1)(u_2 - v_1)}{(v_1 - u_1)(u_2 - v_2)(u_2 - u_1)(v_2 - v_1)} \right)^{c/6(n-1/n)} \mathcal{F}_n(x), \quad (64)$$

where $x = \frac{(v_1 - u_1)(u_2 - v_2)}{(v_2 - u_1)(u_2 - v_1)}$ is again real and now satisfies $-\infty < x < 0$. This can be rewritten in terms of an ordered four point ratio

$$y = \frac{(v_1 - u_1)(v_2 - u_2)}{(u_2 - u_1)(v_2 - v_1)} = \frac{x}{x - 1}, \quad (65)$$

with $0 < y < 1$, as

$$\text{Tr}(\rho_A^{T_2})^n = c_n^2 \left(\frac{(u_2 - u_1)(v_2 - v_1)}{(v_1 - u_1)(v_2 - u_2)(v_2 - u_1)(u_2 - v_1)} \right)^{c/6(n-1/n)} \mathcal{G}_n(y). \quad (66)$$

Equating equations (64) and (66), we can relate the two scaling functions $\mathcal{F}_n(x)$ and $\mathcal{G}_n(y)$ as

$$\mathcal{G}_n(y) = (1 - y)^{c/3(n-1/n)} \mathcal{F}_n\left(\frac{y}{y - 1}\right). \quad (67)$$

Notice that *this relation does not depend on the parity of n* and so, in order to have a non-trivial replica limit $n_e \rightarrow 1$ for the logarithmic negativity

$$\mathcal{E}(y) = \lim_{n_e \rightarrow 1} \ln \mathcal{G}_{n_e}(y) = \lim_{n_e \rightarrow 1} \ln \left[\mathcal{F}_{n_e}\left(\frac{y}{y - 1}\right) \right], \quad (68)$$

some parity effect should appear in the n dependence of the function $\mathcal{F}_n(x)$ for $x < 0$.

The first fundamental consequence of Eq. (68) is that, for conformal invariant systems, the negativity is a scale invariant quantity (i.e. a function only of y) because all the dimensional prefactors cancel in the replica limit. This has been argued already in the literature on the basis of numerical data [11, 12], but never proved.

It is useful to consider the ratio

$$R_n(y) \equiv \frac{\text{Tr}(\rho_A^{T_2})^n}{\text{Tr}(\rho_A)^n} = \frac{\mathcal{G}_n(y)}{\mathcal{F}_n(y)} = (1 - y)^{c/3(n-1/n)} \frac{\mathcal{F}_n(y/(y - 1))}{\mathcal{F}_n(y)}, \quad (69)$$

in which all the prefactors cancel. Being $\lim_{n \rightarrow 1} \text{Tr}(\rho_A)^n = 1$ and $\mathcal{F}_1(y) = 1$ for $0 < y < 1$, we have that the negativity can be obtained just by considering replica limit of this ratio

$$\mathcal{E}(y) = \ln \lim_{n_e \rightarrow 1} R_{n_e}(y). \quad (70)$$

The function $\mathcal{F}_n(x)$ which gives the negativity has been calculated for general integral n only for the free compactified boson [34] and for the critical Ising model [35]. Some other partial results are also known [36, 37, 38, 39, 40, 41, 42, 43, 44, 45, 46, 47, 48, 49, 50, 51, 52]. However, the calculations in Refs. [34, 35] provide the function $\mathcal{F}_n(x)$ only for $0 < x < 1$ and it is a non-trivial technical problem to extend it to the domain $x < 0$ in which we are now interested. Before embarking in these calculations, we discuss some simple and important physical consequences of Eqs. (66), (67), and (68) which are highlighted by considering the limits $y \rightarrow 1$ and $y \rightarrow 0$, i.e. close and far intervals respectively.

5.1. The limit of two very close intervals: $y \rightarrow 1$.

If $u_2 \rightarrow v_1$ then $y \rightarrow 1^-$ and we should recover the previous result for adjacent intervals. Let us denote with $\epsilon = u_2 - v_1$ and $\ell_j = v_j - u_j$ so that Eq. (66) becomes

$$\text{Tr}(\rho_A^{T_2})^n \simeq c_n^2 \left(\frac{1}{(\ell_1 + \ell_2)\epsilon} \right)^{c/6(n-1/n)} \mathcal{G}_n(y), \quad \text{with } y = 1 - \frac{\ell_1 + \ell_2}{\ell_1 \ell_2} \epsilon + O(\epsilon^2). \quad (71)$$

This reduces to the result for adjacent intervals in Eqs. (48) only if

$$\mathcal{G}_n(y) \simeq g_n(1 - y)^{\alpha_n}, \quad (72)$$

with α_n equal to $\Delta_{\mathcal{T}_n^2}$ the dimension of \mathcal{T}_n^2 , i.e.

$$\alpha_n = \begin{cases} \frac{c}{6} \left(\frac{n_e}{2} - \frac{2}{n_e} \right), & \text{if } n = n_e \text{ even,} \\ \frac{c}{12} \left(n_o - \frac{1}{n_o} \right), & \text{if } n = n_o \text{ odd.} \end{cases} \quad (73)$$

We stress that this power-law behavior for y close to 1 is valid apart from possible multiplicative logarithmic corrections, whose precise form should be obtained on a case by case basis.

In the replica limit $n_e \rightarrow 1$, we then have $\lim_{n_e \rightarrow 1} \alpha_{n_e} = -c/4$, i.e. the negativity *diverges* approaching $y = 1$ in the universal way

$$\mathcal{E}(y) = -\frac{c}{4} \ln(1 - y). \quad (74)$$

Clearly for any discrete system with a finite number of degrees of freedom in the two intervals, the negativity will remain finite in the limit of adjacent intervals, i.e. the limit of zero lattice spacing $a \rightarrow 0$ and $y \rightarrow 1$ do not commute (as it is well known when deriving a three-point function from the limit of the four-point one [63]). As it should be clear from the calculation above, this corresponds to set $\epsilon = a$ (no distance can be smaller than the lattice spacing) and not true divergence arises in a finite discrete system. For $n_o \rightarrow 1$, we instead have $\lim_{n_o \rightarrow 1} \alpha_{n_o} = 0$ as it should to obtain the normalization $\text{Tr} \rho_A^{T_2} = 1$.

Furthermore the knowledge of the function $\mathcal{G}_n(y)$ allows to calculate the universal structure constant $C_{\mathcal{T}_n \bar{\mathcal{T}}_n \mathcal{T}_n}$ equating Eqs. (72) and (48), and we obtain (setting $\epsilon = a$)

$$C_{\mathcal{T}_n \bar{\mathcal{T}}_n \mathcal{T}_n} = g_n. \quad (75)$$

5.2. The limit of two very far intervals: $y \rightarrow 0$.

The limit of far intervals $y \rightarrow 0$ can be worked out from the small x expansion of $\mathcal{F}_n(x)$ carried out in full generality in Ref. [35]. This follows from a generalization of operator product expansion (termed short length expansion in [35]) that for the case of the entanglement entropies of two intervals give

$$\text{Tr } \rho_A^n = \frac{c_n^2}{(\ell_1 \ell_2)^{c/6(n-1/n)}} \sum_{\{k_j\}} \left(\frac{\ell_1 \ell_2}{n^2 r^2} \right)^{\sum_j (\Delta_{k_j} + \bar{\Delta}_{k_j})} s_{\{k_j\}}(n), \quad (76)$$

where the sum is over all the sets of possible operators $\{\phi_{k_j}\}$ of the CFT with conformal dimensions $(\Delta_{k_j}, \bar{\Delta}_{k_j})$. $s_{\{k_j\}}(n)$ are calculable coefficients depending on the correlation functions of these operators

$$s_{\{k_j\}}(n) \propto \langle \prod_{j=1}^n \phi_{k_j}(e^{2\pi i j/n}) \rangle_{\mathbb{C}}. \quad (77)$$

All these coefficients $s_{\{k_j\}}(n)$, in the limit $n \rightarrow 1$ (independently of the parity of n) become one-point functions which always vanish in the complex plane. This implies the very strong consequence that the logarithmic negativity $\mathcal{E}(y)$ *vanishes as $y \rightarrow 0$ faster than any power*.

5.3. The function $\mathcal{F}_n(x)$ for $0 < x < 1$.

In order to calculate $\text{Tr}(\rho_A^{T_2})^n$ we first need to report some known results about the function $\mathcal{F}_n(x)$ which has been calculated for the free compactified boson and for the Ising model. In the following we will discuss only the case of the boson.

For a boson compactified on a circle of radius R (a Luttinger liquid field theory), the universal scaling function $\mathcal{F}_n(x)$ for generic integral $n \geq 1$ and for $0 < x < 1$ can be written as [34]

$$\mathcal{F}_n(x) = \frac{\Theta(0|\eta\Gamma) \Theta(0|\Gamma/\eta)}{\Theta(0|\Gamma)^2}, \quad (78)$$

where Γ is an $(n-1) \times (n-1)$ matrix with elements

$$\Gamma_{rs} = \frac{2i}{n} \sum_{k=1}^{n-1} \sin\left(\pi \frac{k}{n}\right) \beta_{k/n} \cos\left[2\pi \frac{k}{n}(r-s)\right], \quad (79)$$

and

$$\beta_y = \frac{F_y(1-x)}{F_y(x)}, \quad F_y(x) \equiv {}_2F_1(y, 1-y; 1; x), \quad (80)$$

η is a universal critical exponent proportional to the square of the compactification radius R , while Θ is the Riemann-Siegel theta function

$$\Theta(0|\Gamma) \equiv \sum_{\mathbf{m} \in \mathbf{Z}^{n-1}} \exp[i\pi \mathbf{m} \cdot \Gamma \cdot \mathbf{m}]. \quad (81)$$

This generalizes the result for $n = 2$ in Ref. [36]. We mention that, although the moments of the reduced density matrix have been obtained for all integer n , the analytic continuation to complex n is still beyond our knowledge and so is the Von Neumann entanglement entropy.

It is also worth to report the first terms in the short length expansion (76) in the case of compactified free boson [35]

$$\mathcal{F}_n(x) = 1 + \left(\frac{x}{4n^2}\right)^\alpha s_2(n) + \left(\frac{x}{4n^2}\right)^{2\alpha} s_4(n) + \dots, \quad (82)$$

where $\alpha = \min[\eta, 1/\eta]$ and

$$s_2(n) = n \left(\frac{x}{4n^2}\right)^\alpha \sum_{j=1}^{n-1} \frac{1}{[\sin(\pi \frac{j}{n})]^{2\alpha}}. \quad (83)$$

Also the coefficient $s_4(n)$ has been explicitly calculated [35]. Both $s_2(n)$ and $s_4(n)$ can be identified with the contributions of the short-length expansion coming from the two- and four-point functions of the most relevant operators in the theory. In the limit $n \rightarrow 1$, independently of the parity of n , we have $s_2(1) = s_4(1) = 0$ as it should, given the general considerations above.

5.4. The function $\mathcal{G}_n(y)$ and the negativity for a non-compactified boson.

Before considering the case of the compactified free boson it is worth to study the simpler and physical limit when the compactification radius diverges. In this case, the limit of Eq. (78) for $\eta \gg 1$ has been worked out in Ref. [34] and it reads for $0 < x < 1$

$$\mathcal{F}_n^{\eta=\infty}(x) = \frac{\eta^{(n-1)/2}}{[\prod_{k=1}^{n-1} F_{k/n}(x) F_{k/n}(1-x)]^{1/2}}. \quad (84)$$

Despite the relative (compared to Eq. (78)) simplicity of this form, many physical ingredients for the calculation of the negativity are already present here.

From Eq. (67) we can write $\mathcal{G}_n(y)$ as

$$\mathcal{G}_n^{\eta=\infty}(y) = (1-y)^{(n-1/n)/3} \frac{\eta^{(n-1)/2}}{[\prod_{k=1}^{n-1} \text{Re}(F_{k/n}(\frac{y}{y-1}) \overline{F}_{k/n}(\frac{1}{1-y}))]^{1/2}}, \quad (85)$$

and the ratio with $\mathcal{F}_n(y)$

$$R_n^{\eta=\infty}(y) = (1-y)^{(n-1/n)/3} \left[\frac{\prod_{k=1}^{n-1} F_{k/n}(y) F_{k/n}(1-y)}{\prod_{k=1}^{n-1} \text{Re}(F_{k/n}(\frac{y}{y-1}) \overline{F}_{k/n}(\frac{1}{1-y}))} \right]^{1/2}, \quad (86)$$

in which the η dependence drops out. The arguments of the hypergeometric functions in the denominator are not in the interval $[0, 1]$ and they should be handled with care to select the proper analytic continuation valid for $x \in [0, 1]$. This can be achieved by using that for $x \in (0, 1)$ and $k/n \neq 1/2$, it holds (see e.g. [53] vol. I, section 2.9, Eqs. (34) and (3))

$$\begin{aligned} F_{k/n}\left(\frac{1}{1-x}\right) &= \frac{\Gamma(1-2k/n)}{\Gamma(1-k/n)^2} e^{-i\pi k/n} (1-x)^{k/n} {}_2F_1\left(\frac{k}{n}, \frac{k}{n}; \frac{2k}{n}; 1-x\right) + (k \rightarrow n-k), \\ F_{k/n}\left(\frac{x}{x-1}\right) &= (1-x)^{k/n} {}_2F_1(k/n, k/n; 1; x). \end{aligned} \quad (87)$$

We stress that these expressions are symmetric under $k \leftrightarrow n-k$. Instead for $k/n = 1/2$ since we have

$$F_{1/2}(z) = \frac{2}{\pi} K(z), \quad (88)$$

where $K(z)$ is the complete elliptic integral of the first kind, we can use the simpler relations

$$F_{1/2}\left(\frac{1}{1-x}\right) = \frac{2}{\pi} \sqrt{1-x} [K(1-x) - iK(x)], \quad (89)$$

$$F_{1/2}\left(\frac{x}{x-1}\right) = \frac{2}{\pi} \sqrt{1-x} K(x), \quad (90)$$

$$\operatorname{Re}\left[F_{1/2}\left(\frac{x}{x-1}\right) \overline{F_{1/2}\left(\frac{1}{1-x}\right)}\right] = \left(\frac{2}{\pi}\right)^2 (1-x) K(x) K(1-x). \quad (91)$$

From Eq. (91) it is clear that the ratio $R_2^{\eta=\infty}(y)$ equals 1 identically, as it should according to Eq. (34).

For $n > 2$, the ratio (86) displays a key mathematical difference between odd and even n . Indeed, each term in the product in both numerator and denominator is invariant under $k \leftrightarrow n-k$ (even if this is not evident from the formulas). Thus, for odd n the products in the numerator and in the denominator are both squares of the products for k up to $(n-1)/2$. For even n this is not true because of the presence of the term $k/n = 1/2$. Nevertheless a simplification occurs between the terms $k/n = 1/2$ in the numerator and in the denominator:

$$\frac{F_{1/2}(y) F_{1/2}(1-y)}{\operatorname{Re}\left[F_{1/2}\left(\frac{y}{y-1}\right) \overline{F_{1/2}\left(\frac{1}{1-y}\right)}\right]} = \frac{1}{1-y}, \quad (92)$$

which is equivalent to $R_2(y) = 1$. Thus we have

$$R_n^{\eta=\infty}(y) = \begin{cases} (1-y)^{\frac{1}{3}(n-\frac{1}{n})} \frac{\prod_{k=1}^{\frac{n-1}{2}} F_{k/n}(y) F_{k/n}(1-y)}{\prod_{k=1}^{\frac{n-1}{2}} \operatorname{Re}\left[F_{k/n}\left(\frac{y}{y-1}\right) \overline{F_{k/n}\left(\frac{1}{1-y}\right)}\right]}, & \text{odd } n, \\ (1-y)^{\frac{1}{3}(n-\frac{1}{n})-\frac{1}{2}} \frac{\prod_{k=1}^{\frac{n}{2}-1} F_{k/n}(y) F_{k/n}(1-y)}{\prod_{k=1}^{\frac{n}{2}-1} \operatorname{Re}\left[F_{k/n}\left(\frac{y}{y-1}\right) \overline{F_{k/n}\left(\frac{1}{1-y}\right)}\right]}, & \text{even } n, \end{cases} \quad (93)$$

Despite of the relative simplicity of this formula for $R_n^{\eta=\infty}(y)$, we did not manage to work out the full analytic continuation to $n_e \rightarrow 1$. However, it is extremely instructive to look at the limit $y \rightarrow 1$ when we can perform the analytic continuation explicitly and understand how the “mode” $k/n = 1/2$ is responsible of the main qualitative differences between n_e even and n_o odd.

5.4.1. The analytic continuation in the limit of close intervals. In order to calculate the analytic continuation to obtain the negativity for $y \rightarrow 1^-$, instead of considering the ratio $R_n^{\eta=\infty}(y)$, it is easier to study the function $\mathcal{G}_n(y)$ in Eq. (85) that we rewrite as

$$\mathcal{G}_n(y) = \eta^{(n-1)/2} (1-y)^{1/3(n-1/n)} D_n(y)^{-1}, \quad (94)$$

with

$$D_n(y) = \left[\prod_{k=1}^{n-1} \operatorname{Re}\left[F_{k/n}\left(\frac{y}{y-1}\right) \overline{F_{k/n}\left(\frac{1}{1-y}\right)}\right] \right]^{1/2}. \quad (95)$$

Each term in the product is invariant for $n \leftrightarrow n-k$, thus we can rewrite it as

$$D_{n_o}(y) = \left[\prod_{k=1}^{(n_o-1)/2} \operatorname{Re}\left[F_{k/n_o}\left(\frac{y}{y-1}\right) \overline{F_{k/n_o}\left(\frac{1}{1-y}\right)}\right] \right], \quad (96)$$

$$D_{n_e}(y) = \frac{2}{\pi}(1-y)^{1/2} \sqrt{K(y)K(1-y)} \left[\prod_{k=1}^{n_e/2-1} \operatorname{Re} \left[F_{k/n_e} \left(\frac{y}{y-1} \right) \bar{F}_{k/n_e} \left(\frac{1}{1-y} \right) \right] \right], \quad (97)$$

where for $n = n_e$ even we isolated the term $k/n = 1/2$ using Eq. (91).

In order to calculate the asymptotic behavior as $y \rightarrow 1^-$, we rewrite each factor in the two products above as

$$\begin{aligned} \operatorname{Re} \left[F_{k/n} \left(\frac{y}{y-1} \right) \bar{F}_{k/n} \left(\frac{1}{1-y} \right) \right] &= (1-y)^{k/n} {}_2F_1(k/n, k/n; 1; y) \\ &\times \left(\frac{\Gamma(1-2k/n)}{\Gamma(1-k/n)^2} (1-y)^{k/n} {}_2F_1\left(\frac{k}{n}, \frac{k}{n}; \frac{2k}{n}; 1-y\right) - (k \leftrightarrow n-k) \right) \cos(\pi k/n). \end{aligned} \quad (98)$$

Then, for the asymptotic behavior of $D_n(y)$ close to $y = 1$ we need

$$\lim_{x \rightarrow 1^-} {}_2F_1(k/n, k/n; 1; x) = \frac{\pi}{\sin(2\pi \frac{k}{n}) \Gamma(1 - \frac{k}{n})^2 \Gamma(\frac{2k}{n})}, \quad \frac{k}{n} < \frac{1}{2}, \quad (99)$$

$$\lim_{x \rightarrow 1^-} K(x) = -\frac{1}{2} \ln(1-x) + 2 \ln 2 + o(1), \quad (100)$$

$$K(0) = \frac{\pi}{2}, \quad {}_2F_1(a, b; c; 0) = 1. \quad (101)$$

For $(1-y) \ll 1$, in Eq. (98) the term $(1-y)^{k/n}$ dominates compared to $(1-y)^{1-k/n}$ (we recall $k/n < 1/2$) which can be neglected.

Thus for odd n , the expansion of (96) as $y \rightarrow 1$ is

$$D_{n_o}(y) = (1-y)^{(n_o-1)/n_o} \prod_{k=1}^{(n_o-1)/2} \frac{\pi \Gamma(1 - \frac{2k}{n_o})}{2 \sin(\pi \frac{k}{n_o}) \Gamma(1 - \frac{k}{n_o})^4 \Gamma(\frac{2k}{n_o})} + \dots, \quad (102)$$

where we used Eq. (98) and $\prod_{k=1}^{(n-1)/2} x^{2k/n} = x^{(n-1)/4}$. After some algebra, we have $\lim_{n_o \rightarrow 1} D_{n_o}(y) = 1$, as it should. Plugging the value of $D_{n_o}(y)$ into Eq. (94), we recover the general expansion for y close to 1 in Eqs. (72) and (73).

For even n , using again Eq. (98) and $\prod_{k=1}^{n/2-1} x^{2k/n} = x^{n/4-1/2}$, we have

$$D_{n_e}(y) = (1-y)^{n_e/4} \sqrt{K(y)} P_{n_e} + \dots, \quad (103)$$

where we defined the constant

$$P_n = \sqrt{\frac{2}{\pi}} \prod_{k=1}^{n/2-1} \frac{\pi \Gamma(1 - \frac{2k}{n})}{2 \sin(\pi \frac{k}{n}) \Gamma(1 - \frac{k}{n})^4 \Gamma(\frac{2k}{n})}, \quad (104)$$

and we left $K(y)$ instead of considering its expansion in Eq. (100), for simplicity in the notations. Plugging $D_{n_e}(y)$ in Eq. (94), we recover the general expansion for y close to 1 of $\mathcal{G}_{n_e}(y) \propto (1-y)^{c/6(n_e/2-2/n_e)}$ up to a logarithmic correction.

For $n_e \rightarrow 1$, we then have

$$D_1(y) = (1-y)^{1/4} \sqrt{K(y)} P_1 + o(1), \quad (105)$$

which gives the desired expansion of the logarithmic negativity for $y \rightarrow 1^-$

$$\begin{aligned} \mathcal{E}(y) &= -\ln D_1(y) = -\frac{1}{4} \ln(1-y) - \frac{1}{2} \ln K(y) - \ln P_1 + o(1) \\ &= -\frac{1}{4} \ln(1-y) - \frac{1}{2} \ln \left(-\frac{1}{2} \ln(1-y) \right) - \ln P_1 + o(1). \end{aligned} \quad (106)$$

(Notice a typo in the published version of Ref. [21] where we wrote the expansion of $e^{\mathcal{E}(y)}$ instead of $\mathcal{E}(y)$). A part from a subleading double-logarithmic correction, this

agrees with the general expansion given in Eq. (74) for the negativity of two intervals when they get closer. Here we can also calculate analytically the constant P_1 .

From the definition of P_n we have

$$\sqrt{\frac{\pi}{2}} P_n \equiv \prod_{k=1}^{n/2-1} \frac{\pi \Gamma(1 - \frac{2k}{n})}{2 \sin(\pi \frac{k}{n}) \Gamma(1 - \frac{k}{n})^4 \Gamma(\frac{2k}{n})} = \prod_{k=1}^{n/2-1} \frac{\pi}{2 \sin(\pi \frac{k}{n}) \Gamma(1 - \frac{k}{n})^4}, \quad (107)$$

where we used $\prod_{k=1}^{n/2-1} [\Gamma(1 - 2k/n) / \Gamma(2k/n)] = 1$ because in the product the same terms appear in opposite order in the numerator and in the denominator. Part of the remaining product is trivial and indeed we have

$$\sqrt{\frac{2}{\pi}} \prod_{k=1}^{n/2-1} \frac{\pi}{2 \sin(\pi k/n)} = \left(\frac{\pi}{2}\right)^{(n-3)/2} \frac{1}{n^{1/2} 2^{(1-n)/2}} \xrightarrow{n \rightarrow 1} \frac{2}{\pi}. \quad (108)$$

The second piece is instead more complicated. Let us consider the product

$$p_n = \prod_{k=1}^{n/2-1} \Gamma(1 - k/n) \Rightarrow \ln p_n = \sum_{k=1}^{n/2-1} \ln \Gamma(1 - k/n). \quad (109)$$

Now we can employ the following integral representation of the logarithm of the Γ function

$$\ln \Gamma(z) = \int_0^\infty \frac{dt e^{-t}}{t} \left(\frac{e^{-(z-1)t} - 1}{1 - e^{-t}} + z - 1 \right), \quad (110)$$

to rewrite

$$\ln p_n = \sum_{k=1}^{n/2-1} \int_0^\infty \frac{dt e^{-t}}{t} \left(\frac{e^{tk/n} - 1}{1 - e^{-t}} - \frac{k}{n} \right), \quad (111)$$

which, inverting the order of sum and integral, can be easily summed up as

$$\ln p_n = \int_0^\infty \frac{dt e^{-t}}{t} \left[\frac{1}{1 - e^{-t}} \left(\frac{e^{t/2} - 1}{e^{t/n} - 1} - \frac{n}{2} \right) - \frac{n-2}{8} \right], \quad (112)$$

whose analytic continuation at $n = 1$ is

$$p_1 = \exp \left(\int_0^\infty \frac{dt e^{-t}}{t} \left[\frac{1}{1 - e^{-t}} \left(\frac{e^{t/2} - 1}{e^t - 1} - \frac{1}{2} \right) + \frac{1}{8} \right] \right) = \frac{A^{3/2}}{2^{1/24} e^{1/8} \pi^{1/4}}, \quad (113)$$

where $A = \exp(1/12 - \zeta'(-1)) = 1.2824\dots$ is Glaishers constant, related to the Riemann zeta function $\zeta(z)$. Putting together Eqs. (107), (108), and (113) we finally have

$$P_1 = \frac{2}{\pi p_1^4} = \frac{2^{7/6} e^{1/2}}{A^6} = 0.832056\dots \quad (114)$$

5.5. The function $\mathcal{G}_n(y)$ and the negativity for the compactified boson.

As discussed in Ref. [34], for a free complex boson whose real and imaginary parts are compactified on a circle of radius R when encircling a branch point, we have the additional freedom of winding around the circle in the target space, i.e. $\phi_j(e^{2\pi i} z, e^{-2\pi i} \bar{z}) = \phi_{j-1}(z, \bar{z}) + 2\pi R(m_{j,1} + im_{j,2})$, where $m_{j,1}, m_{j,2} \in \mathbb{Z}$, if the branch point is in the origin. The integer numbers $m_{i,l}$ can be organized into vectors such as $\mathbf{m}_1 = (m_{1,1}, m_{2,1} \dots m_{n,1})$ or even in $2n$ -dimensional ones

$\mathbf{m} = (m_{1,1}, m_{2,1} \dots m_{n,1}, m_{1,2}, m_{2,2} \dots m_{n,2})$. In all this section we will denote vectors with bold symbols to be easily distinguished from scalars.

The function $\mathcal{F}_n(x, \bar{x})$ appearing in Eq. (58) for a real scalar field is the square root of the same quantity for a complex field because the latter is the sum of two independent real scalar fields. Then, following [34] and using some results in [54, 55], we have that the square of $\mathcal{F}_n(x, \bar{x})$ for a real scalar field and for any four-point ratio $x, \bar{x} \in \mathbb{C}$ is given by

$$[\mathcal{F}_n(x, \bar{x})]^2 = \prod_{k=1}^n \frac{\text{const}}{F_{k/n}(x) \bar{F}_{k/n}(1 - \bar{x}) + \bar{F}_{k/n}(\bar{x}) F_{k/n}(1 - x)} \sum_{\mathbf{m}^{(1)}, \mathbf{m}^{(2)}} \prod_{k=1}^n e^{-S_{k/n}^{\text{cl}}}, \quad (115)$$

where the sum runs over the possible integer components of $\mathbf{m}^{(1)}, \mathbf{m}^{(2)} \in (\mathbb{Z} + i\mathbb{Z})^n = \mathbb{Z}^{2n}$ and where the constant does not depend on x and it will be fixed later on. The dependence on the compactification radius is encoded in the “classical action” $S_{k/n}^{\text{cl}}$ first calculated in Ref. [54]:

$$S_{k/n}^{\text{cl}} = \frac{2g\pi \sin(\pi k/n)}{n} \left[\frac{|\tau_{k/n}|^2}{\beta_{k/n}} |\xi_1|^2 + \frac{\alpha_{k/n}}{\beta_{k/n}} (\xi_1 \bar{\xi}_2 \bar{\gamma} + \bar{\xi}_1 \xi_2 \gamma) + \frac{|\xi_2|^2}{\beta_{k/n}} \right], \quad (116)$$

where g is the Lagrangian coupling $\mathcal{L}[\phi_j] = g|\nabla\phi_j|^2/(4\pi)$ and $\gamma \equiv -ie^{-i\pi k/n}$ and ξ_p ($p = 1, 2$) are

$$\xi_p = 2\pi R \sum_{l=1}^n (\theta_{k/n})^l (m_{l,1}^{(p)} + i m_{l,2}^{(p)}), \quad \theta_{k/n} \equiv e^{2\pi i k/n}. \quad (117)$$

The dependence on the harmonic ratio x in Eq. (59) is instead encoded in the quantity $\tau_{k/n}$ also derived in Ref. [54]:

$$\tau_{k/n} = i \frac{F_{k/n}(1 - x)}{F_{k/n}(x)} \equiv \alpha_{k/n} + i\beta_{k/n}, \quad (118)$$

being $\alpha_{k/n}$ and $\beta_{k/n}$ the real and the imaginary part of $\tau_{k/n}$ respectively. Before embarking in the main calculation, we stress that the crucial difference compared to the case of real x with the constraint $0 \leq x \leq 1$, considered in Ref. [34], is the presence of the linear term in γ and $\bar{\gamma}$ in Eq. (116) which was vanishing because $\alpha_{k/n} = 0$ for $0 \leq x \leq 1$.

The products involving ξ_p in Eq. (116) can be written as

$$\begin{aligned} \frac{\xi_p \bar{\xi}_q}{(2\pi R)^2} &= \sum_{r,s=1}^n (\tilde{C}_{k/n})_{rs} [m_{r,1}^{(p)} m_{s,1}^{(q)} + m_{r,2}^{(p)} m_{s,2}^{(q)}] - (\tilde{S}_{k/n})_{rs} [m_{r,2}^{(p)} m_{s,1}^{(q)} - m_{r,1}^{(p)} m_{s,2}^{(q)}] \\ &+ i \left[(\tilde{S}_{k/n})_{rs} [m_{r,1}^{(p)} m_{s,1}^{(q)} + m_{r,2}^{(p)} m_{s,2}^{(q)}] + (\tilde{C}_{k/n})_{rs} [m_{r,2}^{(p)} m_{s,1}^{(q)} - m_{r,1}^{(p)} m_{s,2}^{(q)}] \right], \end{aligned} \quad (119)$$

where we introduced the $n \times n$ real matrices $\tilde{C}_{k/n}$ and $\tilde{S}_{k/n}$ whose elements are

$$(\tilde{C}_{k/n})_{rs} \equiv \cos\left(2\pi \frac{k}{n}(r - s)\right), \quad (\tilde{S}_{k/n})_{rs} \equiv \sin\left(2\pi \frac{k}{n}(r - s)\right), \quad (120)$$

with $r, s = 1, \dots, n$. Notice that $\tilde{C}_{k/n}$ is symmetric and $\tilde{S}_{k/n}$ is antisymmetric. Plugging (119) into (116) and summing over k , as required in (115), we obtain

$$\sum_{k=1}^n S_{k/n}^{\text{cl}} = \frac{8gR^2\pi^3}{n} \sum_{r,s=1}^n \sum_{k=1}^n \sin\left(\pi \frac{k}{n}\right) \left\{ \frac{|\tau_{k/n}|^2}{\beta_{k/n}} (\tilde{C}_{k/n})_{rs} \left(m_{r,1}^{(1)} m_{s,1}^{(1)} + m_{r,2}^{(1)} m_{s,2}^{(1)} \right) \right.$$

$$\begin{aligned}
& -\frac{2\alpha_{k/n}}{\beta_{k/n}} \left[\cos\left(\pi\frac{k}{n}\right) (\tilde{S}_{k/n})_{rs} \left(m_{r,1}^{(1)} m_{s,1}^{(2)} + m_{r,2}^{(1)} m_{s,2}^{(2)} \right) \right. \\
& \quad \left. + \sin\left(\pi\frac{k}{n}\right) (\tilde{C}_{k/n})_{rs} \left(m_{r,1}^{(1)} m_{s,1}^{(2)} + m_{r,2}^{(1)} m_{s,2}^{(2)} \right) \right] \\
& + \frac{1}{\beta_{k/n}} (\tilde{C}_{k/n})_{rs} \left(m_{r,1}^{(2)} m_{s,1}^{(2)} + m_{r,2}^{(2)} m_{s,2}^{(2)} \right) \Big\}, \tag{121}
\end{aligned}$$

where many terms of $S_{k/n}^{\text{cl}}$ vanish in the sum over k because they are odd under $k \leftrightarrow n-k$. Introducing the $2n$ vectors of integers $\tilde{\mathbf{m}}_1 \equiv (\mathbf{m}_1^{(1)}, \mathbf{m}_1^{(2)})$ and $\tilde{\mathbf{m}}_2 \equiv (\mathbf{m}_2^{(1)}, \mathbf{m}_2^{(2)})$ made respectively by the real and the imaginary parts of $\mathbf{m}^{(1)}$ and $\mathbf{m}^{(2)}$, it is possible to rewrite Eq. (121) as

$$-\sum_{k=1}^n S_{k/n}^{\text{cl}} = i\pi\eta \left(\tilde{\mathbf{m}}_1^t \cdot \tilde{G} \cdot \tilde{\mathbf{m}}_1 + \tilde{\mathbf{m}}_2^t \cdot \tilde{G} \cdot \tilde{\mathbf{m}}_2 \right), \quad \tilde{\mathbf{m}}_1, \tilde{\mathbf{m}}_2 \in \mathbb{Z}^{2n}, \tag{122}$$

where $\eta \propto R^2$. The matrix \tilde{G} is symmetric, purely imaginary and it can be written in terms of $n \times n$ block matrices as

$$\tilde{G} \equiv 2i \begin{pmatrix} \tilde{A} & \tilde{W} \\ \tilde{W}^t & \tilde{B} \end{pmatrix}, \tag{123}$$

with

$$\tilde{A} = \frac{1}{n} \sum_{k=1}^n \frac{|\tau_{k/n}|^2}{\beta_{k/n}} \sin(\pi k/n) \tilde{C}_{k/n} = \sum_{k=1}^n \frac{|\tau_{k/n}|^2}{\beta_{k/n}} \sin(\pi k/n) \tilde{E}_{k/n}, \tag{124}$$

$$\tilde{B} = \frac{1}{n} \sum_{k=1}^n \frac{1}{\beta_{k/n}} \sin(\pi k/n) \tilde{C}_{k/n} = \sum_{k=1}^n \frac{1}{\beta_{k/n}} \sin(\pi k/n) \tilde{E}_{k/n}, \tag{125}$$

$$\begin{aligned}
\tilde{W} &= -\frac{1}{n} \sum_{k=1}^n \frac{\alpha_{k/n}}{\beta_{k/n}} \sin(\pi k/n) \left[\sin(\pi k/n) \tilde{C}_{k/n} + \cos(\pi k/n) \tilde{S}_{k/n} \right] \\
&= -\sum_{k=1}^n \frac{\alpha_{k/n}}{\beta_{k/n}} \sin(\pi k/n) \left[\sin(\pi k/n) - i \cos(\pi k/n) \right] \tilde{E}_{k/n}, \tag{126}
\end{aligned}$$

where we introduced the complex matrices $\tilde{E}_{k/n}$ for $k = 1, \dots, n$ whose elements are

$$(\tilde{E}_{k/n})_{rs} \equiv e^{2\pi i(k/n)(r-s)}/n. \tag{127}$$

These are hermitian matrices satisfying $\tilde{E}_{p/n} \cdot \tilde{E}_{q/n} = \delta_{p,q} \tilde{E}_{p/n}$, therefore they are projectors, a property which guarantees that \tilde{A} , \tilde{B} and \tilde{W} commute. Since \tilde{A} and \tilde{B} are symmetric, \tilde{G} is symmetric by construction. The eigenvalues of \tilde{A} , \tilde{B} and \tilde{W} are respectively

$$a_k = \frac{|\tau_{k/n}|^2}{\beta_{k/n}} \sin\left(\pi\frac{k}{n}\right), \quad b_k = \frac{1}{\beta_{k/n}} \sin\left(\pi\frac{k}{n}\right), \quad w_k = i \frac{\alpha_{k/n}}{\beta_{k/n}} \sin\left(\pi\frac{k}{n}\right) e^{i\pi k/n}, \tag{128}$$

where $k = 1, \dots, n$. Most of these eigenvalues are degenerate because of the symmetry $k \leftrightarrow n-k$. Since \tilde{A} , \tilde{B} and \tilde{W} commute, the characteristic polynomial of \tilde{G} is

$$\begin{aligned}
P(\lambda) &= \det \left[(\tilde{A} - \lambda \mathbb{I}_n)(\tilde{B} - \lambda \mathbb{I}_n) - \tilde{W} \cdot \tilde{W}^t \right] \\
&= \det \left(\sum_{k=1}^n \left[(a_k - \lambda)(b_k - \lambda) - |w_k|^2 \right] \tilde{E}_{k/n} \right) = \prod_{k=1}^n \left[(a_k - \lambda)(b_k - \lambda) - |w_k|^2 \right], \tag{129}
\end{aligned}$$

which is obtained from the fact that the matrices $\tilde{E}_{k/n}$ are projectors. Then the eigenvalues of \tilde{G} are

$$\lambda_k^\pm = \frac{1}{2} \left(a_k + b_k \pm \sqrt{(a_k - b_k)^2 + 4|w_k|^2} \right) \quad (130)$$

$$= \frac{\sin(\pi k/n)}{2\beta_{k/n}} \left(|\tau_{k/n}|^2 + 1 \pm \sqrt{(|\tau_{k/n}|^2 + 1)^2 - 4\beta_{k/n}^2} \right). \quad (131)$$

They are all real and strictly positive for $k \in \{1, \dots, n-1\}$, while $\lambda_n^\pm = 0$. We also have $\lambda_k^\pm = \lambda_{n-k}^\pm$ for the invariance $k \leftrightarrow n-k$ of (128). Thus, 0 is always a doubly degenerate eigenvalue. As for the degeneracy of the remaining positive eigenvalues, if $n-1$ is even then they are all doubly degenerate as well; instead if $n-1$ is odd then they are all doubly degenerate except for $\lambda_{n/2}^\pm$ which are non degenerate.

From the common eigenvectors of \tilde{A} , \tilde{B} and \tilde{W} , we can construct the $2n \times 2n$ matrix \tilde{U} diagonalizing \tilde{G}

$$\tilde{G} = \tilde{U} \cdot \left(\begin{array}{c|c} \begin{matrix} \lambda_1^+ & & & \\ & \ddots & & \\ & & \lambda_{n-1}^+ & \\ \hline & & & 0 \end{matrix} & \begin{matrix} \\ \\ \\ \end{matrix} \\ \hline \begin{matrix} \\ \\ \\ \end{matrix} & \begin{matrix} \lambda_1^- & & & \\ & \ddots & & \\ & & \lambda_{n-1}^- & \\ & & & 0 \end{matrix} \end{array} \right) \cdot \tilde{U}^{-1}. \quad (132)$$

Since \tilde{G} has zero eigenvalues, the sum over the vectors $\mathbf{m}^{(j)}$ in Eq. (115) is divergent. Thus, as done in [34], we introduce a regularized \tilde{G}_ϵ by replacing the two zeros on the diagonal of the diagonal matrix in (132) with a small cutoff $\epsilon > 0$. This allows us to write the regularized sum in (115) in terms of a Riemann Siegel theta function

$$\sum_{\tilde{\mathbf{m}}_1, \tilde{\mathbf{m}}_2 \in \mathbb{Z}^{2n}} \exp \left[i\pi\eta \left(\tilde{\mathbf{m}}_1^\dagger \cdot \tilde{G}_\epsilon \cdot \tilde{\mathbf{m}}_1 + \tilde{\mathbf{m}}_2^\dagger \cdot \tilde{G}_\epsilon \cdot \tilde{\mathbf{m}}_2 \right) \right] = \Theta(0|\eta\tilde{G}_\epsilon)^2, \quad (133)$$

where the regularized \tilde{G}_ϵ can be written as

$$\tilde{G}_\epsilon = \tilde{G} + \frac{\epsilon}{n} \begin{pmatrix} I_n & 0_n \\ 0_n & I_n \end{pmatrix}, \quad (134)$$

where I_n and 0_n are $n \times n$ matrices with all equal elements given by 1 and 0 respectively. Now we can isolate the divergent factor by observing that the limit

$$\lim_{\epsilon \rightarrow 0} [n\epsilon\Theta(0|\eta\tilde{G}_\epsilon)] = \Theta(0|\eta\tilde{G}), \quad (135)$$

gives a finite result. Since the divergent part is independent of x , it can be adsorbed into a normalization constant. The $2(n-1) \times 2(n-1)$ symmetric matrix G introduced in the r.h.s. of (135) is

$$G \equiv 2i \begin{pmatrix} A & W \\ W^\dagger & B \end{pmatrix}, \quad (136)$$

where

$$A = \frac{1}{n} \sum_{k=1}^{n-1} \frac{|\tau_{k/n}|^2}{\beta_{k/n}} \sin(\pi k/n) C_{k/n} = \sum_{k=1}^{n-1} \frac{|\tau_{k/n}|^2}{\beta_{k/n}} \sin(\pi k/n) E_{k/n}, \quad (137)$$

$$B = \frac{1}{n} \sum_{k=1}^{n-1} \frac{1}{\beta_{k/n}} \sin(\pi k/n) C_{k/n} = \sum_{k=1}^{n-1} \frac{1}{\beta_{k/n}} \sin(\pi k/n) E_{k/n}, \quad (138)$$

$$\begin{aligned} W &= -\frac{1}{n} \sum_{k=1}^{n-1} \frac{\alpha_{k/n}}{\beta_{k/n}} \sin(\pi k/n) [\sin(\pi k/n) C_{k/n} + \cos(\pi k/n) S_{k/n}] \\ &= -\sum_{k=1}^{n-1} \frac{\alpha_{k/n}}{\beta_{k/n}} \sin(\pi k/n) [\sin(\pi k/n) - i \cos(\pi k/n)] E_{k/n}. \end{aligned} \quad (139)$$

These matrices are obtained from the corresponding tilded ones given in Eqs. (124), (125) and (126) by removing the last column and the last row, namely

$$(C_{k/n})_{rs} \equiv (\tilde{C}_{k/n})_{rs}, \quad (S_{k/n})_{rs} \equiv (\tilde{S}_{k/n})_{rs}, \quad (E_{k/n})_{rs} \equiv (\tilde{E}_{k/n})_{rs}, \quad (140)$$

with $r, s = 1, \dots, n-1$. Absorbing the divergent part into the normalization constant, we can finally write (115) as

$$[\mathcal{F}_n(x, \bar{x})]^2 = \text{const} \frac{\Theta(0|\eta G)^2}{\prod_{k=1}^{n-1} [F_{k/n}(x) \bar{F}_{k/n}(1-\bar{x}) + \bar{F}_{k/n}(\bar{x}) F_{k/n}(1-x)]}. \quad (141)$$

As first check, for real x we have $\alpha_{k/n} = 0$ for every k and therefore the off diagonal blocks W in G are zero. In this case the Riemann theta function $\Theta(0|\eta G)$ factorizes into a product of two Riemann theta functions and (141) reproduces the result of [34], as it should.

As for the normalization constant in (141), since it is independent of x , it is given by the one computed in [34], namely $(2\eta)^{n-1}$. Thus, for the real compactified free boson, we find that

$$\mathcal{F}_n(x, \bar{x}) = \frac{\eta^{(n-1)/2} \Theta(0|\eta G)}{\sqrt{\prod_{k=1}^{n-1} \text{Re}(F_{k/n}(x) \bar{F}_{k/n}(1-\bar{x}))}} = \frac{\eta^{(n-1)/2} \Theta(0|\eta G)}{\prod_{k=1}^{n-1} |F_{k/n}(x)| \sqrt{\text{Im}(\tau_{k/n}(x))}}, \quad (142)$$

where we used that $\text{Re}(F_{k/n}(x) \bar{F}_{k/n}(1-\bar{x})) = |F_{k/n}(x)|^2 \text{Im}(\tau_{k/n}(x))$. In the limit of non compactified boson $\eta \rightarrow \infty$ the Riemann-Siegel theta function does not contribute because $\Theta(0|\eta G) \rightarrow 1$, recovering the results for the non-compactified boson. Notice also that for $\eta = 1$, while for x real and $x \in [0, 1]$ we have $\mathcal{F}_n(x, \bar{x}) = 1$ [34], this is not true for general complex x and, in particular, for x real and negative.

From Eqs. (67) and (142) we can write $\mathcal{G}_n(y)$ for $0 < y < 1$ as

$$\mathcal{G}_n(y) = (1-y)^{(n-1/n)/3} \frac{\eta^{\frac{n-1}{2}}}{[\prod_{k=1}^{n-1} \text{Re}(F_{k/n}(\frac{y}{y-1}) \bar{F}_{k/n}(\frac{1}{1-y}))]^{1/2}} \Theta\left(0|\eta G\left(\frac{y}{y-1}\right)\right). \quad (143)$$

Unfortunately, we are not able to compute the analytic continuation of $\mathcal{G}_{n_e}(y)$ to $n_e \rightarrow 1$ which gives the logarithmic negativity for the free compactified boson. This reflects a similar problem for the standard Rényi entropies which are also known only for integer $n > 2$.

5.5.1. Invariance of $\mathcal{F}_n(x, \bar{x})$ for $x \leftrightarrow 1-x$ and for $\eta \leftrightarrow 1/\eta$. For real x , it turned out that $\mathcal{F}_n(x)$ was invariant under $x \leftrightarrow 1-x$. In order to show this invariance also for complex x , we focus on Eq. (141) in which the denominator is clearly invariant. As for its numerator $\Theta(0|\eta G)$, it is also invariant because when $x \leftrightarrow 1-x$ we have

$$\tau_{k/n} \rightarrow -\frac{1}{\tau_{k/n}} \quad \Longleftrightarrow \quad \alpha_{k/n} \rightarrow -\frac{\alpha_{k/n}}{|\tau_{k/n}|^2}, \quad \beta_{k/n} \rightarrow \frac{\beta_{k/n}}{|\tau_{k/n}|^2}, \quad (144)$$

leading to

$$A \rightarrow B, \quad W \rightarrow -W. \quad (145)$$

This change does not modify the sum defining $\Theta(0|\eta G)$. Indeed, it can be reabsorbed by a redefinition of the sign of the first half (or, equivalently, of the second half) of the vector of integers over which we are summing.

The function $\mathcal{F}_n(x, \bar{x})$ in (142) is also invariant under $\eta \leftrightarrow 1/\eta$. Indeed, by employing the Poisson summation formula, we can rewrite (142) in a form where this invariance is manifest, namely

$$\mathcal{F}_n(x, \bar{x}) = \frac{\Theta(0|T)}{\prod_{k=1}^{n-1} |F_{k/n}(x)|}, \quad (146)$$

where the $2(n-1) \times 2(n-1)$ symmetric matrix T is

$$T = \begin{pmatrix} i\eta \mathcal{I} & \mathcal{R} \\ \mathcal{R} & i\mathcal{I}/\eta \end{pmatrix}, \quad (147)$$

and the $(n-1) \times (n-1)$ symmetric matrices \mathcal{I} and \mathcal{R} are

$$\mathcal{I} = \frac{2}{n} \sum_{k=1}^{n-1} \beta_{k/n} \sin(\pi k/n) C_{k/n} = 2 \sum_{k=1}^{n-1} \beta_{k/n} \sin(\pi k/n) E_{k/n}, \quad (148)$$

$$\mathcal{R} = \frac{2}{n} \sum_{k=1}^{n-1} \alpha_{k/n} \sin(\pi k/n) C_{k/n} = 2 \sum_{k=1}^{n-1} \alpha_{k/n} \sin(\pi k/n) E_{k/n}. \quad (149)$$

Writing the quadratic form in the exponent of the generic term of the sum defining $\Theta(0|T)$, it is straightforward to see that (146) is invariant under $\eta \leftrightarrow 1/\eta$. The matrices (148) and (149) are respectively the imaginary and the real part of the matrix

$$\tau = \mathcal{R} + i\mathcal{I} = \frac{2}{n} \sum_{k=1}^{n-1} \tau_{k/n} \sin(\pi k/n) C_{k/n} = 2 \sum_{k=1}^{n-1} \tau_{k/n} \sin(\pi k/n) E_{k/n}. \quad (150)$$

We can write $\Theta(0|T)$ in (146) also as

$$\Theta(0|T) = \sum_{\mathbf{p}, \tilde{\mathbf{p}}} \exp \left[i\pi (\mathbf{p}^t \cdot \tau \cdot \mathbf{p} - \tilde{\mathbf{p}}^t \cdot \bar{\tau} \cdot \tilde{\mathbf{p}}) \right] \quad (151)$$

where

$$(\mathbf{p}, \tilde{\mathbf{p}}) = \left(\frac{\mathbf{n}}{\sqrt{2\eta}} + \frac{\mathbf{m}\sqrt{2\eta}}{2}, \frac{\mathbf{n}}{\sqrt{2\eta}} - \frac{\mathbf{m}\sqrt{2\eta}}{2} \right), \quad \mathbf{n}, \mathbf{m} \in \mathbb{Z}^{n-1}. \quad (152)$$

Comparing with the results in the literature [56], from (151) we conclude that τ is the period matrix of the genus $g = n-1$ Riemann surface we are dealing with. For $x \in (0, 1)$ we have that $\alpha_{k/n} = 0$ and therefore all the elements of the matrix \mathcal{R} vanish identically. In this case $\Theta(0|T) = \Theta(0|i\eta\mathcal{I})\Theta(0|i\mathcal{I}/\eta)$ and the $\eta \leftrightarrow 1/\eta$ invariant expression found in [34] is recovered.

5.5.2. *The special case $n = 2$ for the compactified boson.* It is instructive to analyze the details of the case $n = 2$ with complex x . Now the Riemann surface is a torus and the period matrix reduces to a number: its modulus $\tau_{1/2}(x)$. First we recall that

$$F_{1/2}(x) = \frac{2}{\pi} K(x) = \theta_3(\tau_{1/2})^2, \quad (153)$$

where $K(x)$ is the complete elliptic integral of the first kind and

$$\tau_{1/2}(x) = i \frac{K(1-x)}{K(x)}, \quad x(\tau_{1/2}) = \left(\frac{\theta_2(\tau_{1/2})}{\theta_3(\tau_{1/2})} \right)^4. \quad (154)$$

For $n = 2$ we have that $\mathcal{T}_2 = \overline{\mathcal{T}}_2$. From Eqs. (58), (146), and (153) we find that the four point function of the twist fields \mathcal{T}_2 for the compactified real boson reads

$$\begin{aligned} \langle \mathcal{T}_2(z_1) \mathcal{T}_2(z_2) \mathcal{T}_2(z_3) \mathcal{T}_2(z_4) \rangle &= \left| \frac{z_{31} z_{42}}{z_{21} z_{32} z_{41} z_{43}} \right|^{1/4} \frac{\Theta(0|T)}{|\theta_3(\tau_{1/2})|^2} \\ &= \left| \frac{1}{z_{21} z_{31} z_{41} z_{32} z_{42} z_{43} [x(1-x)]^2} \right|^{1/12} \frac{\Theta(0|T)}{|\theta_3(\tau_{1/2})|^2}, \end{aligned} \quad (155)$$

where T is the 2×2 matrix given by (147) for $n = 2$, namely

$$T = \begin{pmatrix} i\eta\beta_{1/2} & \alpha_{1/2} \\ \alpha_{1/2} & i\beta_{1/2}/\eta \end{pmatrix}. \quad (156)$$

From (154) and the identity $\theta_4^4 = \theta_3^4 - \theta_2^4$ one can find that

$$x(1-x) = \left(\frac{\theta_2(\tau_{1/2}) \theta_4(\tau_{1/2})}{\theta_3(\tau_{1/2})^2} \right)^4. \quad (157)$$

The transformation properties of the Jacobi theta functions lead also to the following identities (here $\tau = \tau_{1/2}$)

$$x(-1/\tau) = 1 - x(\tau), \quad x\left(\frac{-\tau}{\tau-1}\right) = \frac{1}{x(\tau)}, \quad x(\tau+1) = \frac{x(\tau)}{x(\tau)-1}. \quad (158)$$

Plugging (157) into (155), we find

$$\begin{aligned} \langle \mathcal{T}_2(z_1) \mathcal{T}_2(z_2) \mathcal{T}_2(z_3) \mathcal{T}_2(z_4) \rangle &= \left| \frac{1}{z_{21} z_{31} z_{41} z_{32} z_{42} z_{43}} \right|^{1/12} \frac{\Theta(0|T)}{|\theta_2(\tau_{1/2}) \theta_3(\tau_{1/2}) \theta_4(\tau_{1/2})|^{2/3}} \\ &= \left| \frac{1}{z_{21} z_{31} z_{41} z_{32} z_{42} z_{43}} \right|^{1/12} \frac{\Theta(0|T)}{2^{1/3} |\eta(\tau_{1/2})|^2}, \end{aligned} \quad (159)$$

where in the last step we used the identity $2\eta^3 = \theta_2\theta_3\theta_4$ and $\eta(z)$ is the Dedekind eta function, which should not be confused with the compactification parameter. Now we observe that $\mathcal{Z}_2(\tau_{1/2}) \equiv \Theta(0|T)/|\eta(\tau_{1/2})|^2$ is the partition function of the compactified boson on the torus (see e.g. Eq. (10.62) of [63] with $\eta_{\text{here}} = R_{\text{there}}^2/2$).

Let us consider the exchanges $z_1 \leftrightarrow z_3$, $z_2 \leftrightarrow z_3$ and $z_3 \leftrightarrow z_4$ separately. From (59) it is easy to see that they correspond to the following involutions: $x \leftrightarrow 1-x$, $x \leftrightarrow 1/x$ and $x \leftrightarrow x/(x-1)$ respectively. From (158), one notices that they are also associated some $SL(2, \mathbb{Z})$ transformations of $\tau_{1/2}$. Since the prefactor containing the z_{ij} 's in (159) is invariant under the three exchanges above and the partition function $\mathcal{Z}_2(\tau_{1/2})$ is $SL(2, \mathbb{Z})$ invariant [63], we conclude that the four point function (159) is

invariant under $z_1 \leftrightarrow z_3$, $z_2 \leftrightarrow z_3$ and $z_3 \leftrightarrow z_4$ separately. This allows us to find that the ratio defined in (69) for the compactified boson is given by

$$R_2(y) = 1 \quad (160)$$

identically for $0 < y < 1$. However, we stress that, ultimately, this is just the fact that $\mathcal{T}_2 = \bar{\mathcal{T}}_2$.

6. Systems with boundaries

Let us consider a 1D system on the semi-infinite line, say $[0, \infty)$ and a bipartition $A_2 = [0, \ell]$ and A_1 the reminder. We then have

$$\begin{aligned} \text{Tr}(\rho_A^{T_2})^{n_e} &= \langle \mathcal{T}_{n_e}^2(\ell) \rangle = \tilde{c}_{n_e/2}^2 \left(\frac{2\ell}{a} \right)^{-c/6(n_e/2-2/n_e)}, \\ \text{Tr}(\rho_A^{T_2})^{n_o} &= \langle \mathcal{T}_{n_o}^2(\ell) \rangle = \tilde{c}_{n_o}^2 \left(\frac{2\ell}{a} \right)^{-c/12(n_o-1/n_o)}, \\ \mathcal{E} &= \frac{c}{4} \ln \frac{2\ell}{a} + 2 \ln \tilde{c}_{1/2}. \end{aligned} \quad (161)$$

The non-universal constants \tilde{c}_n are not the same as those appearing in the case of the infinite system c_n , but are related to them via the Affleck-Ludwig boundary entropy [32] as discussed in Refs. [22, 33].

Like for a periodic system, in the case of a finite system of length L with the same boundary conditions on both ends, the negativity can be obtained by a simple logarithmic mapping which results in the net replacement $\ell \rightarrow \frac{L}{\pi} \sin(\pi\ell/L)$ and we get

$$\mathcal{E} = \frac{c}{4} \ln \left[\frac{2L}{\pi a} \sin \left(\frac{\pi\ell}{L} \right) \right] + 2 \ln \tilde{c}_{1/2}. \quad (162)$$

The case of two adjacent finite intervals (or even one interval not adjacent to a boundary) is a two-point function in the half-plane, which has the same complexity as a four-point function in the full plane and then depends on the full operator content and not only on the central charge, as for the case of two disjoint intervals on the full line. However, some results can be achieved in a quite general way.

Let us first consider the case of two adjacent intervals, the first one starting from the boundary, i.e. $A_1 = [0, \ell_1]$ and $A_2 = [\ell_1 + \ell_2]$ where $B = [\ell_1 + \ell_2, \infty)$ is the remainder. We place the spatial coordinate along the imaginary direction in the complex plane, while the imaginary time is on the real direction, i.e. $z = \tau + ix$, thus the system lies on the upper half plane (UHP). The traces of integer powers of the partial transpose reduced density matrix, correspond to the UHP two-point function

$$\text{Tr}(\rho_A^{T_2})^n = \langle \bar{\mathcal{T}}_n^2(z_1) \mathcal{T}_n(z_2) \rangle_{\text{UHP}}, \quad \text{with } z_1 = i\ell_1, \quad z_2 = i(\ell_1 + \ell_2). \quad (163)$$

The general form of such two-point function can be obtained by images method and it is [67]

$$\langle \bar{\mathcal{T}}_n^2(z_1) \mathcal{T}_n(z_2) \rangle_{\text{UHP}} \propto \frac{\mathcal{F}_n^b(y)}{|z_{1\bar{1}}|^{\Delta_{\mathcal{T}_n^2}} |z_{2\bar{2}}|^{\Delta_{\mathcal{T}_n}}}, \quad y = \frac{z_{12} z_{\bar{1}\bar{2}}}{z_{1\bar{2}} z_{\bar{1}2}}, \quad (164)$$

where $z_{\bar{i}} = \bar{z}_i$, $z_{ij} = z_i - z_j$, y is the four point ratio built with the two points and their images, and $\mathcal{F}_n^b(y)$ is a scale invariant function of y . Calculating this function is complicated, but there are some general conclusions which can be drawn without

making any calculation. Indeed, let us assume $\ell_1 = \ell_2 = \ell$. In this case $y = 1/9$ is constant, independent of ℓ , as the physical intuition suggests. Then we have

$$\langle \overline{\mathcal{T}}_n(i\ell) \mathcal{T}_n(i2\ell) \rangle_{\text{UHP}} \propto \frac{1}{\ell \Delta \tau_n^2 \ell \Delta \tau_n}. \quad (165)$$

Using the values of $\Delta \tau_n^2$ in Eqs. (44) and (45), we have

$$\text{Tr}(\rho_A^{T_2})^n \propto \begin{cases} \ell^{-c/6(n-1/n)} & n \text{ odd}, \\ \ell^{-c/12(n-1/n)-c/6(n/2-2/n)} & n \text{ even}. \end{cases} \quad (166)$$

In particular, the n dependence for $n = n_e$ even is quite peculiar, being different from others found before. In the limit $n_e \rightarrow 1$, we obtain

$$\mathcal{E} = \frac{c}{4} \ln \ell + \text{const}, \quad (167)$$

which however is similar to what found in other circumstances. We stress that in the case of a finite system of length L , the result above applies if and only if one scales L with ℓ in such a way to keep fixed the four-point ratio y . In all other circumstances, one should use the full formula with the unknown function $\mathcal{F}_n^b(y)$.

As a last example we mention the case of A_2 being a single interval detached from the boundary and A_1 the remaining part of the half-line. In such a case, ρ_A corresponds to a pure system and so the general result $\mathcal{E} = S_{A_2}^{(1/2)}$ in Eq. (23) applies and the results for the Rényi entropies discussed in Refs. [34, 68] apply straightforwardly.

7. The harmonic chain

In this section we present accurate numerical checks of our CFT predictions for the harmonic chain with periodic and Dirichlet boundary conditions. The Hamiltonian of the harmonic chain with N lattice sites and with nearest neighbor interaction (but the procedure is easily generalized to arbitrary interactions) is

$$H = \sum_{n=0}^{N-1} \left[\frac{1}{2M} p_n^2 + \frac{M\omega^2}{2} q_n^2 + \frac{K}{2} (q_{n+1} - q_n)^2 \right], \quad (168)$$

where periodic boundary conditions correspond to $q_N = q_0$ (and $p_N = p_0$) while Dirichlet boundary conditions to $q_0 = q_N = p_0 = p_N = 0$ (these are sometimes called fixed wall conditions). The variables p_n and q_n satisfy standard commutation relations $[q_n, q_m] = [p_n, p_m] = 0$ and $[q_n, p_m] = i\delta_{nm}$.

The chain is defined by the three parameters ω, K, M , however not all of them are essential. Indeed, we can use a canonical transformation

$$(q_n, p_n) \rightarrow ((MK)^{1/4} q_n, p_n / (MK)^{1/4}), \quad (169)$$

to eliminate one of the three parameters. Introducing $a = \sqrt{M/K}$ then we can rewrite the Hamiltonian as

$$H = \sum_{n=0}^{N-1} \left[\frac{1}{2a} p_n^2 + \frac{a\omega^2}{2} q_n^2 + \frac{1}{2a} (q_{n+1} - q_n)^2 \right]. \quad (170)$$

In this form, it is evident that the Hamiltonian is the lattice discretization of a free-boson (Klein Gordon field) with lattice spacing a and mass ω . Indeed in the limit $a \rightarrow 0$, $N \rightarrow \infty$, with $Na = L$, we can replace

$$q_n \rightarrow \phi(x), \quad \frac{p_n}{a} \rightarrow \pi(x) = \dot{\phi}(x), \quad \text{with } x = na, \quad (171)$$

(satisfying $[\phi(x), \pi(x')] = i\delta(x - x')$ with $\delta_{n,n'} \rightarrow a\delta(x - x')$) and the Hamiltonian above reduces to the two-dimensional euclidean action

$$S = \frac{1}{2} \int_0^L dx \int d\tau [(\partial_\mu \phi)^2 + \omega^2 \phi^2]. \quad (172)$$

For $\omega = 0$ the theory is critical and conformal with central charge the $c = 1$. The boson field $\phi(x)$ is not compactified and so the theory corresponds to the limit $\eta \rightarrow \infty$ in the previous CFT description.

7.1. Diagonalization and correlation functions of the harmonic chain with periodic boundary conditions.

For periodic boundary conditions, the Hamiltonian (168) can be diagonalized by exploiting the translational invariance and introducing the Fourier transforms of the canonical variables, namely

$$q_r = \frac{1}{\sqrt{N}} \sum_{k=0}^{N-1} \tilde{q}_k e^{2\pi i k r / N}, \quad \tilde{q}_k = \frac{1}{\sqrt{N}} \sum_{s=0}^{N-1} q_s e^{-2\pi i k s / N}, \quad (173)$$

(and similarly for p_r) for $r = 1, \dots, N$. The Hamiltonian (168) then becomes

$$H = \sum_{k=0}^{N-1} \left(\frac{1}{2M} \tilde{p}_k \tilde{p}_{N-k} + \frac{M\omega_k^2}{2} \tilde{q}_k \tilde{q}_{N-k} \right), \quad (174)$$

where

$$\omega_k \equiv \sqrt{\omega^2 + \frac{4K}{M} \sin\left(\frac{\pi k}{N}\right)^2} \geq \omega, \quad k = 0, \dots, N-1. \quad (175)$$

Notice that $\omega_{-k} = \omega_{N-k} = \omega_k$. As usual, we identify \tilde{p}_{N-k} with \tilde{p}_{-k} and \tilde{q}_{N-k} with \tilde{q}_{-k} . The minimum values assumed by the dispersion relation ω_k 's is $\omega_0 = \omega$. From the canonical commutation relation $[q_r, p_s] = i\delta_{rs}$, one finds that \tilde{q}_k and \tilde{p}_{N-k} are canonically conjugate (i.e. $[\tilde{q}_k, \tilde{p}_{-k'}] = i\delta_{k,k'}$). Now one defines the annihilation and creation operators as

$$a_k \equiv \sqrt{\frac{M\omega_k}{2}} \left(\tilde{q}_k + \frac{i}{M\omega_k} \tilde{p}_k \right), \quad a_k^\dagger \equiv \sqrt{\frac{M\omega_k}{2}} \left(\tilde{q}_{-k} - \frac{i}{M\omega_k} \tilde{p}_{-k} \right), \quad (176)$$

which satisfy the algebra $[a_k, a_{k'}] = [a_k^\dagger, a_{k'}^\dagger] = 0$ and $[a_k, a_{k'}^\dagger] = i\delta_{k,k'}$. Then the Hamiltonian (174) becomes

$$H = \sum_{k=0}^{N-1} \omega_k \left(a_k^\dagger a_k + \frac{1}{2} \right). \quad (177)$$

The ground state of the harmonic chain is then the vacuum $|0\rangle$ of the a_k , satisfying $a_k|0\rangle = 0$ for any k .

The two point functions $\langle q_r q_s \rangle$ and $\langle p_r p_s \rangle$ in the vacuum are worked out writing $(\tilde{q}_k, \tilde{p}_k)$ in terms of the operators a_k and a_k^\dagger , finding

$$\begin{aligned} \langle 0 | q_r q_s | 0 \rangle &= \frac{1}{2N} \sum_{k=0}^{N-1} \frac{1}{M\omega_k} \cos \left[\frac{2\pi k(r-s)}{N} \right], \\ \langle 0 | p_r p_s | 0 \rangle &= \frac{1}{2N} \sum_{k=0}^{N-1} M\omega_k \cos \left[\frac{2\pi k(r-s)}{N} \right]. \end{aligned} \quad (178)$$

These correlation functions can be organized in correlation matrices \mathbb{Q} and \mathbb{P} whose elements are the correlation functions, i.e.

$$\mathbb{Q}_{rs} \equiv \langle 0|q_r q_s|0\rangle, \quad \mathbb{P}_{rs} \equiv \langle 0|p_r p_s|0\rangle, \quad (179)$$

satisfying $\mathbb{Q} \cdot \mathbb{P} = \mathbb{I}_N/4$, where \mathbb{I}_N is the $N \times N$ identity matrix. We also have $\langle 0|q_r p_s|0\rangle = i\delta_{r,s}/2$.

It is very important for what follows to stress that $\langle 0|q_r q_s|0\rangle$ is not well defined when $\omega = 0$ because $\omega_0 = 0$. This is the well known problem arising from the *zero mode*, i.e. a constant translational invariant field configuration. For $\omega > 0$ we can isolate the term in Eq. (178) which diverges as $\omega \rightarrow 0$

$$\langle 0|q_r q_s|0\rangle = \frac{1}{2NM\omega} + \frac{1}{2N} \sum_{k=1}^{N-1} \frac{1}{M\omega_k} \cos\left[\frac{2\pi k(r-s)}{N}\right], \quad (180)$$

and the remaining sum is finite also in the limit $\omega \rightarrow 0$. For $\omega = 0$, the zero mode leads to divergent expressions, thus we work at finite but small ω such that $\omega L \ll 1$.

7.2. Diagonalization and correlation functions of the harmonic chain with Dirichlet boundary condition.

For the Dirichlet boundary conditions, the diagonalization cannot be performed by Fourier transform because of the breaking of translational invariance. However, we can simply use the Fourier sine transform, defining as in Ref. [62]

$$\tilde{q}_k = \sqrt{\frac{2}{N}} \sum_{r=1}^{N-1} q_r \sin\left(\frac{\pi k r}{N}\right), \quad q_r = \sqrt{\frac{2}{N}} \sum_{k=1}^{N-1} \tilde{q}_k \sin\left(\frac{\pi k r}{N}\right), \quad (181)$$

(and similarly for p_r) with $r = 1, \dots, N-1$. In this basis the Hamiltonian is diagonal

$$H = \sum_{k=1}^{N-1} \left(\frac{1}{2M} \tilde{p}_k^2 + \frac{M\tilde{\omega}_k^2}{2} \tilde{q}_k^2 \right), \quad (182)$$

where the dispersion relation reads

$$\tilde{\omega}_k \equiv \sqrt{\omega^2 + \frac{4K}{M} \sin^2\left(\frac{\pi k}{2N}\right)} > \omega, \quad k = 1, \dots, N-1. \quad (183)$$

The key difference with respect to the periodic case is that $\tilde{\omega}_k > \omega \geq 0$ for $k = 1, \dots, N-1$. Thus, in this model all the quantities are well defined even for $\omega = 0$. In terms of the creation and the annihilation operators, the Hamiltonian takes the form (177) but with $\tilde{\omega}_k$ replacing ω_k .

The correlators in the ground-state of the Hamiltonian are

$$\begin{aligned} \langle 0|q_r q_s|0\rangle &= \frac{1}{N} \sum_{k=1}^{N-1} \frac{1}{M\tilde{\omega}_k} \sin\left(\frac{\pi k r}{N}\right) \sin\left(\frac{\pi k s}{N}\right) = \mathbb{Q}_{rs}, \\ \langle 0|p_r p_s|0\rangle &= \frac{1}{N} \sum_{k=1}^{N-1} M\tilde{\omega}_k \sin\left(\frac{\pi k r}{N}\right) \sin\left(\frac{\pi k s}{N}\right) = \mathbb{P}_{rs}, \end{aligned} \quad (184)$$

where $r, s = 1, \dots, N$.

For these Dirichlet boundary conditions we can write down exact closed formulas for $\omega = 0$ and in the thermodynamic limit $N \rightarrow \infty$, when the correlators (184) become

$$\begin{aligned}\langle 0|q_r q_s|0\rangle &= \frac{1}{2\pi\sqrt{MK}} \left(\psi(1/2 + r + s) - \psi(1/2 + r - s) \right), \\ \langle 0|p_r p_s|0\rangle &= \frac{2\sqrt{MK}}{\pi} \left(\frac{1}{4(r+s)^2 - 1} - \frac{1}{4(r-s)^2 - 1} \right),\end{aligned}\quad (185)$$

where $\psi(z)$ is the digamma function.

7.3. The reduced density matrix and its partial transpose.

The construction of the reduced density matrix ρ_A for the ground-state of the harmonic chain has been detailed in several papers with slightly different theoretical approaches [57, 10, 58, 59, 60, 61]. Following Refs. [58, 61], we can easily relate ρ_A to the correlation matrices $\mathbb{Q}_{rs} = \langle q_r q_s \rangle$ and $\mathbb{P}_{rs} = \langle p_r p_s \rangle$ (derived above for periodic and Dirichlet boundary conditions) restricted to the part A of the system both if the subsystem is connected or formed by an arbitrary number of pieces. Indeed, since the ground-state is Gaussian in normal coordinates (provided that no normal frequency vanishes) the reduced density matrix for an arbitrary subsystem A can be written in the Gaussian form [58, 61]

$$\rho_A \propto \exp \left(- \sum_{j \in A} \epsilon_j b_j^\dagger b_j \right), \quad (186)$$

where b_j^\dagger and b_j are bosonic creation and annihilation operators related to the original operator in the subsystem by a canonical transformation. At this point it is straightforward to fix the value of the ϵ_j by imposing that the correlation functions of q 's and p 's in A calculated with ρ_A equal the ground state ones (e.g. the one calculated above for periodic and Dirichlet boundary conditions). Denoting with \mathbb{P}_A and \mathbb{Q}_A the restriction of the matrices \mathbb{P} and \mathbb{Q} to the subsystem A and with μ_j^2 ($j = 1 \dots \ell$, with ℓ the number of sites in A , not necessarily connected) the eigenvalues of the matrix $\mathbb{P}_A \cdot \mathbb{Q}_A$, i.e.

$$\text{Spectrum}(\mathbb{Q}_A \cdot \mathbb{P}_A) = \{\mu_1^2, \dots, \mu_\ell^2\}, \quad (187)$$

one finds $\mu_j = \frac{1}{2} \coth \frac{\epsilon_j}{2}$ [58]. (Alternatively one could work with the $2\ell \times 2\ell$ matrix formed by two-point functions of position and momentum operators, called reduced covariance matrix. Its reduction to a diagonal form is related to the problem of finding the symplectic spectrum of a symmetric and positive definite matrix [10, 59].)

From the eigenvalues μ_j , using the explicit form of ρ_A above, we obtain the Rényi entropies

$$\text{Tr} \rho_A^n = \prod_{j=1}^{\ell} \left[\left(\mu_j + \frac{1}{2} \right)^n - \left(\mu_j - \frac{1}{2} \right)^n \right]^{-1}, \quad (188)$$

and the entanglement entropy as

$$S_A = \sum_{j=1}^{\ell} \left[\left(\mu_j + \frac{1}{2} \right) \ln \left(\mu_j + \frac{1}{2} \right) - \left(\mu_j - \frac{1}{2} \right) \ln \left(\mu_j - \frac{1}{2} \right) \right]. \quad (189)$$

The partial transpose of the reduced density matrix has been constructed in Ref. [10], where it has been shown that the partial transposition with respect to the

subsystem A_2 has the net effect of changing the sign of the momenta corresponding to the subsystem A_2 , leaving the partial transpose reduced density matrix $\rho_A^{T_2}$ a Gaussian matrix of the form (186). This means that we can simply replace the matrix \mathbb{P}_A with a matrix in which all the momenta in A_2 have been changed sign, i.e.

$$\mathbb{P}_A^{T_2} = \mathbb{R}_{A_2} \mathbb{P}_A \mathbb{R}_{A_2}, \quad (190)$$

where \mathbb{R}_{A_2} is the $\ell \times \ell$ diagonal matrix having -1 in correspondence of the sites belonging to A_2 and $+1$ otherwise, i.e. $(\mathbb{R}_{A_2})_{rs} = \delta_{rs}(-1)^{\delta_{r \in A_2}}$. Notice that $\mathbb{P}_A^{T_1} = \mathbb{P}_A^{T_2}$ because $\mathbb{R}_{A_1} = -\mathbb{R}_{A_2}$. Then the eigenvalues ν_j of the product $\mathbb{Q}_A \cdot \mathbb{P}_A^{T_2}$ determine the full spectrum of $\rho_A^{T_2}$. Denoting

$$\text{Spectrum}(\mathbb{Q}_A \cdot \mathbb{P}_A^{T_2}) = \{\nu_1^2, \dots, \nu_\ell^2\}, \quad (191)$$

we have

$$\text{Tr}(\rho_A^{T_2})^n = \prod_{j=1}^{\ell} \left[\left(\nu_j + \frac{1}{2} \right)^n - \left(\nu_j - \frac{1}{2} \right)^n \right]^{-1}, \quad (192)$$

and the trace norm

$$\|\rho_A^{T_2}\| = \prod_{j=1}^{\ell} \left[\left| \nu_j + \frac{1}{2} \right| - \left| \nu_j - \frac{1}{2} \right| \right]^{-1} = \prod_{j=1}^{\ell} \max \left[1, \frac{1}{2\nu_j} \right]. \quad (193)$$

From this quantity we easily get the negativity \mathcal{N} and the logarithmic negativity \mathcal{E} . Notice that only $\nu_j < 1/2$ contribute to (193).

Let us then summarize the practical procedure to find the negativity and $\text{Tr}(\rho_A^{T_2})^n$ for an arbitrary tripartition $A_1 \cup A_2 \cup B$ in the ground-state of an harmonic chain:

- From the correlation matrices \mathbb{Q} and \mathbb{P} (which for periodic and Dirichlet boundary conditions are given in Eqs. (178) and (184) respectively), construct the reduced correlation matrices \mathbb{Q}_A and \mathbb{P}_A by erasing the rows and columns corresponding to the part B of the system.
- Change the signs of the momenta in the part A_2 to construct the matrix $\mathbb{P}_A^{T_2}$ as in Eq. (190).
- Calculate the eigenvalues ν_j^2 of the product $\mathbb{Q}_A \cdot \mathbb{P}_A^{T_2}$.
- Use Eq. (192) to calculate $\text{Tr}(\rho_A^{T_2})^n$ and Eq. (193) to obtain the negativity from ν_j .

In the semi-analytic calculations presented in the following we will always work in units $M = K = a = 1$ and so the total length is $L = Na = N$.

7.4. The negativity for one interval.

We consider here the case when A_1 is a block of ℓ consecutive sites and A_2 the remainder, i.e. $B \rightarrow \emptyset$, as shown in the bottom of Fig. 1. In this case, the negativity and the traces $\text{Tr}(\rho^{T_2})^n$ coincide with the Rényi entropies for any pure state (cf. Eq. (21)) as proved in Sec. (2.3). It is however important to report these results for a twofold reason. On the one hand, knowing a priori the final result of the calculation provides a non-trivial check of the numerical procedure which indeed differs substantially when calculating $\text{Tr}(\rho^{T_2})^n$ and $\text{Tr}\rho_2^n$ since for latter there is no need neither of a partial transposition, nor of the correlation matrices in the part A_1 (that involves basically the same procedure for one and two intervals). On the other

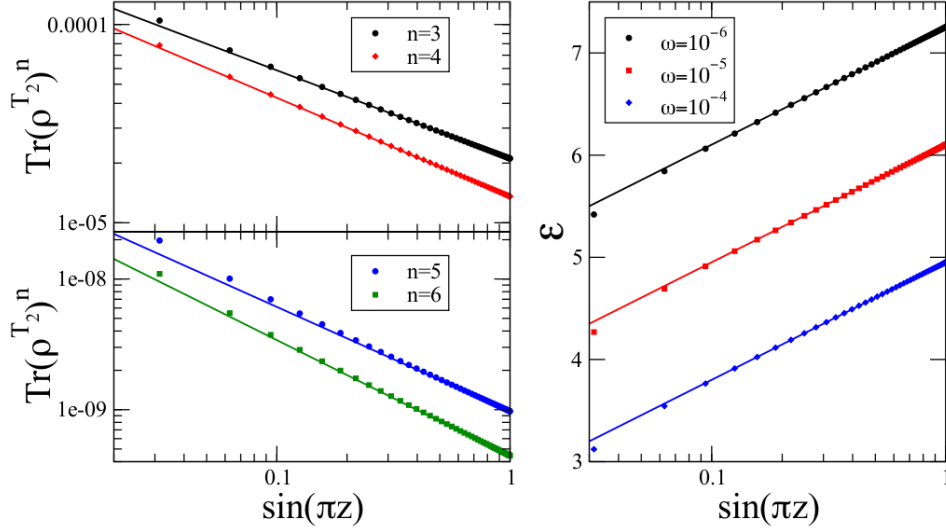


Figure 6. Entanglement in a periodic chain of total length $L = 100$. We consider the bipartition between an interval of length ℓ and the remainder. Here $z = \ell/L$. Left: $\text{Tr}(\rho^{T_2})^n$ for $n = 3, 4, 5, 6$ as function of $\sin(\pi z)$. The straight lines are the CFT predictions where the only free parameter is the overall amplitude c_n (cf. Eqs. (53) and (54)). Right: The logarithmic negativity \mathcal{E} vs the CFT prediction (55). The three curves correspond to different values of ω and show the influence of the zero mode. Indeed they are parallel (in log-linear scale) and the zero mode affects only the non-universal additive constant.

hand, these controlled calculations give also an idea of the corrections to the scaling to the asymptotic CFT formulas.

In the case of periodic boundary conditions, we cannot work directly with $\omega = 0$, because of the zero mode. Thus, we consider several values of ω imposing the further constraint $\omega L \ll 1$ to ensure that all the data for any $1 < \ell < L$ are in the conformal regime. The data for $\text{Tr}(\rho^{T_2})^n$ in the periodic harmonic chain are reported in Fig. 6 for $n = 3, 4, 5, 6$. The agreement with the conformal predictions in Eq. (54) is excellent. The visible deviations for small ℓ are the corrections to the scaling to the entanglement Rényi entropy discussed in Ref. [64, 65, 66] of the unusual form ℓ^{-2/n_R} where n_R is the index of the corresponding Rényi entropy (i.e. $n_R = n$ for n odd and $n_R = n/2$ for n even).

In Fig. 6 we report also the logarithmic negativity as function of the chord length, finding a perfect agreement with the conformal prediction (55). We report the data for three different values of ω , all satisfying $\omega L \ll 1$ and so in the conformal regime. It is evident that in logarithmic-linear scale the three curves are parallel confirming that the zero mode only affects the value of the non-universal additive constant and not the leading logarithmic behavior of \mathcal{E} with the subsystem sizes.

We then perform the same analysis for a finite system of total length L with Dirichlet boundary conditions considering the interval A_1 starting from the boundary up to ℓ and A_2 the remaining $L - \ell$ sites. In this case, as discussed above, there is no zero mode and we can work directly at $\omega = 0$. The data for $\text{Tr}(\rho^{T_2})^n$ are reported in Fig. 7 for several values of n , all for $L = 200$. It is evident that increasing ℓ the data approach the CFT predictions in Eq. (161), but in this case

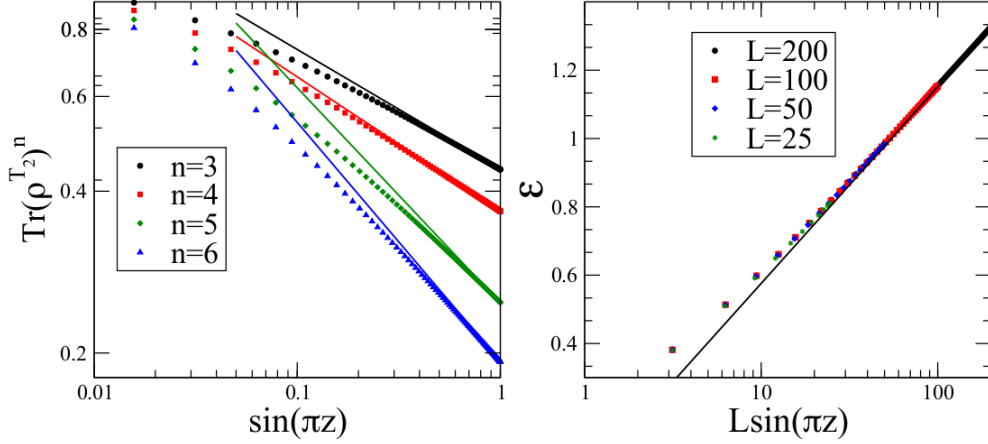


Figure 7. Entanglement in a critical ($\omega = 0$) harmonic chain with Dirichlet boundary conditions of total length L . We consider the bipartition between the interval $A_1 = [0, \ell]$ and the remainder $A_2 = [\ell, L]$. Here $z = \ell/L$. Left: $\text{Tr}(\rho^{T_2})^n$ for $n = 3, 4, 5, 6$ and for $L = 200$ as function of $\sin(\pi z)$. The straight lines are the CFT predictions where the only free parameter is the overall amplitude \tilde{c}_n (cf. Eq. (161)). Right: The logarithmic negativity \mathcal{E} for $L = 25, 50, 100, 200$. The four sets of data collapse on the same curve when plotted against the chord length, as they should.

the corrections to the scaling are much larger than in the periodic case. This does not come unexpected, indeed in Refs. [64, 65, 68] it has been shown that in the presence of the boundaries the corrections to the asymptotic results are of the form ℓ^{-1/n_R} (where again n_R is the index of the corresponding Rényi entropy), i.e. they have an exponent which is half of the corresponding one for periodic systems. On the right of Fig. 7 we report the logarithmic negativity as function of the chord length $L \sin(\pi \ell/L)$ for $L = 25, 50, 100, 200$. All the data at different L collapse on the same curve that for large enough chord length are perfectly described by the CFT prediction (162). The corrections to the scaling are smaller than the ones for $n \geq 2$, in agreement with the general analysis of the Rényi entropies [64, 65, 68].

Finally, we checked that all the results reported in this subsection satisfy the relations in Eq. (21) between $\text{Tr}(\rho^{T_2})^n$ (and \mathcal{E}) and the Rényi entropies in the same state.

7.5. The negativity for two adjacent intervals in periodic chains.

We now consider the case of two adjacent intervals in a periodic system of total length L . For simplicity we consider the two intervals to have equal length ℓ , thus all the results depend on the single parameter $z \equiv \ell/L \in [0, 1/2]$. In terms of z , the CFT predictions in Eqs. (56) can be rewritten as (we fix $c = 1$)

$$\text{Tr}(\rho_A^{T_2})^n \propto \begin{cases} (\sin(\pi z))^{-(n_e/2 - 2/n_e)/3} (\sin(2\pi z))^{-(n_e/2 + 1/n_e)/6}, \\ (\sin^2(\pi z) \sin(2\pi z))^{-(n_o - 1/n_o)/12}, \end{cases} \quad (194)$$

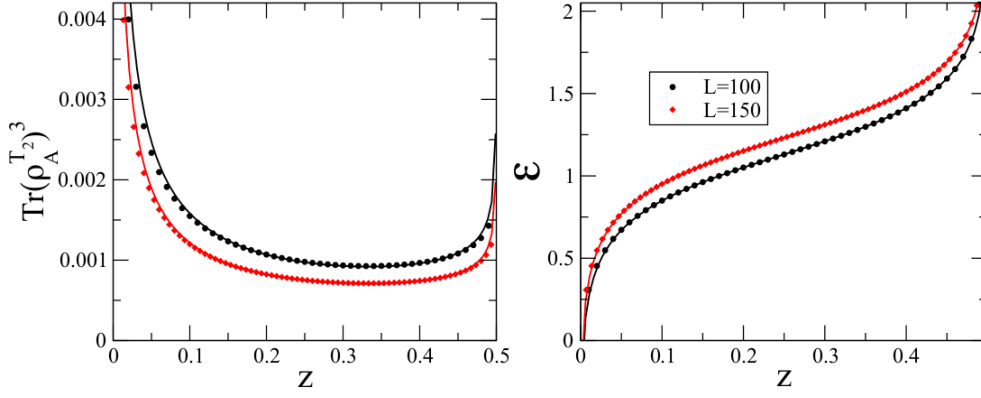


Figure 8. A typical example of the entanglement of two adjacent intervals of the same length ℓ in a periodic chain of length L . The legend refers to both plots and we fix $\omega = 10^{-6}$. Left: $\text{Tr}(\rho_A^{T_2})^3$ as function of $z = \ell/L$. The data are consistent with the conformal prediction (full lines with only one multiplicative free parameter). Right: Logarithmic negativity \mathcal{E} for the same chains as on the left. Again the data are perfectly consistent with the CFT predictions (full lines with only one additive free parameter).

and the proportionality constants depend on L in a known manner. For the logarithmic negativity from Eq. (57), we have

$$\mathcal{E} = \frac{1}{4} \ln \frac{\sin^2(\pi z)}{\sin(2\pi z)} + \text{cnst} = \frac{1}{4} \ln[\tan(\pi z)] + \text{cnst}, \quad (195)$$

where again the additive constant depends on L in a known manner. These predictions are checked against the numerical data in Fig. 8 where the only free parameters in each curve is fixed by a fit. The agreement is clearly excellent.

However one can do even better checks of the theory by constructing ratios in which all the dependence on non-universal parameters (such as those coming from the zero mode) and also the dependence on L cancel. A straightforward idea would be to divide $\text{Tr}(\rho_A^{T_2})^n$ for the value it assumes at a given fixed ℓ , e.g. $\ell = L/4$, i.e. by considering the logarithm of the ratio

$$r_n(z) = \ln \frac{\text{Tr}(\rho_A^{T_{A_2=\ell}})^n}{\text{Tr}(\rho_A^{T_{A_2=L/4}})^n}, \quad (196)$$

whose parameter free CFT predictions for n even and odd are

$$r_{n_e} = \frac{1}{6} \left(\frac{2}{n_e} - \frac{n_e}{2} \right) \ln(2 \sin^2(\pi z)) - \frac{1}{6} \left(\frac{n_e}{2} + \frac{1}{n_e} \right) \ln(\sin(2\pi z)), \quad (197)$$

$$r_{n_o} = \frac{1}{12} \left(\frac{1}{n_o} - n_o \right) \ln(2 \sin^2(\pi z) \sin(2\pi z)). \quad (198)$$

These ratios are shown in Fig. 9 for $n = 3$ and $n = 4$. The agreement of the numerical data and the CFT prediction is excellent. Some very small deviations are visible for z close to 0 and $1/2$, but we checked that they go to zero increasing L in a controllable way.

For the logarithmic negativity, we can analogously define the subtracted quantity

$$\epsilon(z) = \mathcal{E}(\ell, L) - \mathcal{E}(L/4, L) = \frac{1}{4} \ln[\tan(\pi z)], \quad (199)$$

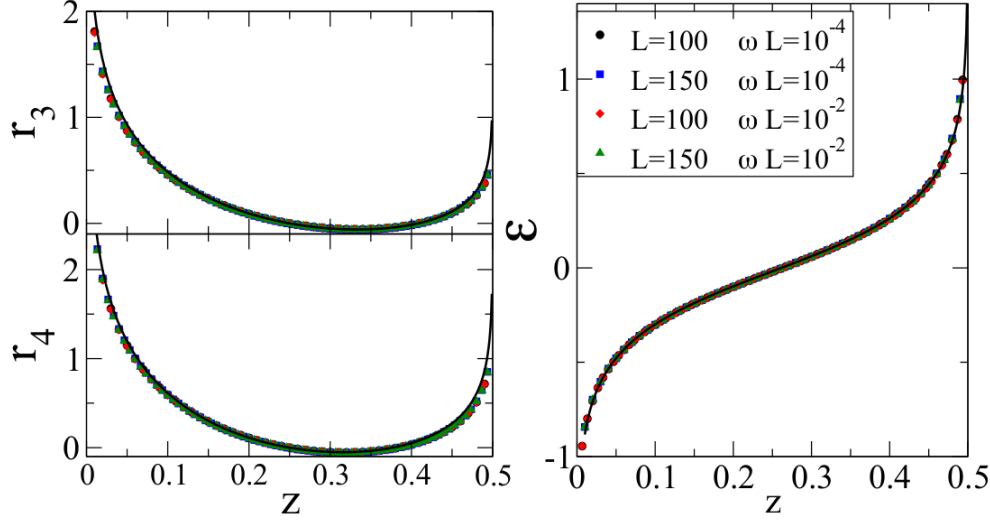


Figure 9. Entanglement for two adjacent intervals of equal length $\ell < L/2$ in a periodic chain of length L . Left: the ratio $r_n(z)$ in Eq. (196) as function of $z = \ell/L$ compared with the parameter free CFT prediction. Right: Subtracted negativity $\epsilon(z)$ in Eq. (199) again compared with the parameter free CFT prediction.

and again the rhs is a parameter free CFT prediction. In Fig. 9 (left panel), this prediction is compared with the numerical data and the agreement is extremely good since no deviations are visible even close to the boundaries.

7.6. The negativity for two disjoint intervals in the periodic chain.

To conclude our analysis of the periodic chain we consider now the most difficult situation of two disjoint intervals for which the negativity has been already considered numerically [12]. Here we start by considering the traces $\text{Tr}(\rho_A^{T_2})^n$ which, in the conformal regime $\omega L \ll 1$, should be described by Eq. (66) with $\mathcal{G}_n(y)$ given in (84). The direct numerical data, that we do not present here, agree well with the CFT predictions where the overall constant is fixed by a fit and explicitly depends on the values of ω and L , since the data are influenced by the zero mode. However, while this is a further confirmation of the predictive power of CFT, it gives not much information on the true entanglement (which is only obtained in the limit $n_e \rightarrow 1$). Indeed the function $\mathcal{G}_n(y)$ turns out to be very close to a constant (in proper units equals 1) and the direct data mainly probe the prefactor to $\mathcal{G}_n(y)$ in Eq. (66), whose logarithm vanishes in the replica limit $n_e \rightarrow 1$, and so does not give any contribution to the negativity.

As already stated in Sec. (5), a practical way to get rid of the prefactor is to consider the ratio $R_n(y)$ in Eq. (69), where also the non-universal parts due to the zero mode cancel and we are left with a universal function of y . The CFT prediction for this ratio $R_n^{\eta=\infty}(y)$ in Eq. (86) is compared to the numerical data in Fig. 10. As L increases, the data approach the CFT result. The differences with the asymptotic formula are due to the presence of unusual corrections to the scaling [64, 65] whose leading part is of the form $L^{-2/n}$. A quantitative finite size scaling analysis is reported

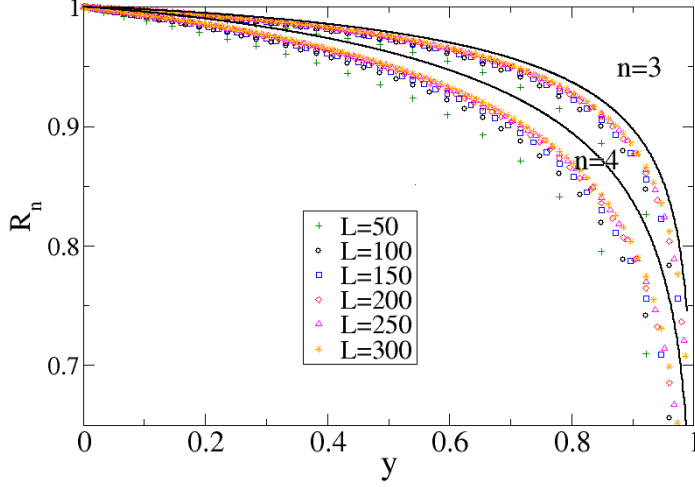


Figure 10. For a periodic chain of length L , we report the ratio $R_n(y)$ defined in Eq. (69) as function of y for several L and for $n = 3, 4$. The continuous lines are the parameter free CFT predictions to which the data converges for $L \rightarrow \infty$.

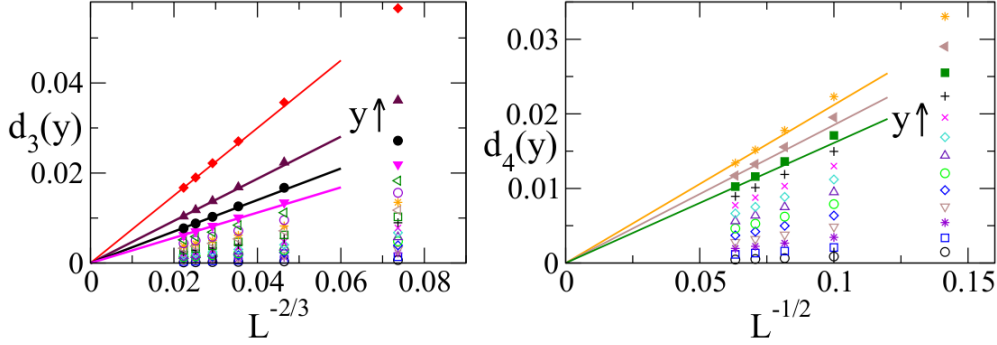


Figure 11. Finite size scaling analysis for $d_n(y)$ in Eq. (200) for $n = 3$ (left) and $n = 4$ (right). We report from Fig. 10 several values of y (increasing in the direction of the arrow, but we do not give the actual value to simplify the reading of the plot). The data are compatible with a leading correction to the scaling of the form $L^{-2/n}$.

in Fig. 11 for $n = 3, 4$ showing that the difference

$$d_n(y) \equiv R_n(y) - R_n^{\eta=\infty}(y), \quad (200)$$

for several values of y is of the expected form $L^{-2/n}$. As well known (even analytically) for other simpler cases [64, 66] for larger n , the subleading corrections to the scaling, of the form $L^{-2p/n}$ with p integer, cannot be neglected and a proper analysis requires the introduction of some fitting parameters.

Finally we turn to the study of the negativity \mathcal{E} reported in Fig. 12 showing that all data collapse on a single curve, without sizable corrections. Unfortunately we do not have the analytic continuation of $R_{n_e}^{\eta=\infty}(y)$ to $n_e \rightarrow 1$ as a function of y . However we can study the two interesting regimes of far and close intervals corresponding to

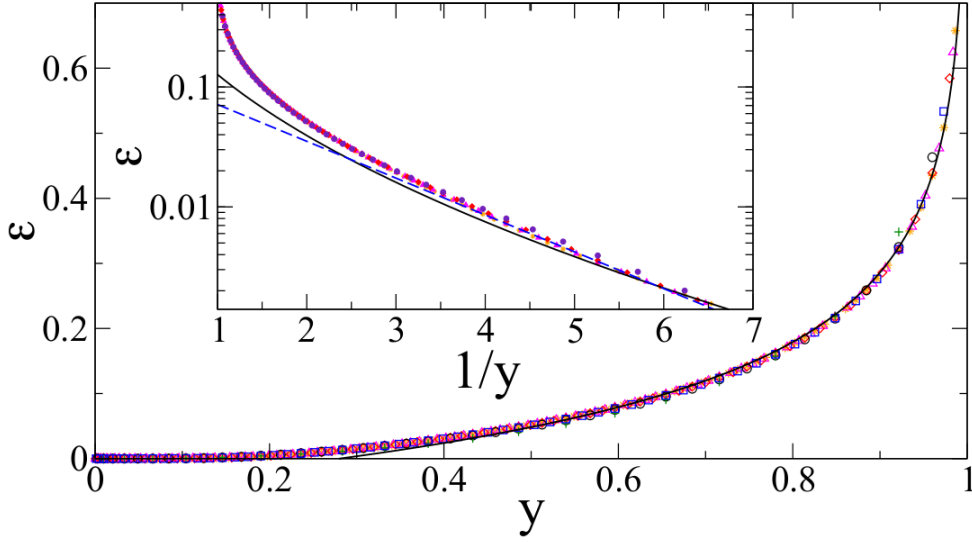


Figure 12. The negativity $\mathcal{E}(y)$ is a universal scale invariant function with an essential singularity at $y = 0$. We report the data for $L = 50, 100, 150, 200, 250, 300$ but, since they are hardly distinguishable, we do not give a legend box. The solid line is the expansion close to $y \sim 1$ in Eq. (202) which very surprisingly describes well the data down to $y \sim 0.3$. The inset shows the same plot in logarithmic scale showing that for small y the two possibilities $\mathcal{E} \sim e^{-a/y}$ and $\mathcal{E} \sim e^{-b/\sqrt{y}}$ are too close to be distinguished.

$y \rightarrow 0$ and $y \rightarrow 1^-$ respectively. For small y , the data, being very close to zero, are consistent with the prediction that they vanish faster than any power. In Ref. [12], on the basis of the numerical data, the form $e^{-a/\sqrt{y}}$ has been proposed. This proposal is shown in logarithmic scale on the inset of Fig. 12 together with a simple exponential $e^{-b/y}$. The two possible scenarios are very difficult to be distinguished on the basis of the numerical calculations involving exponentially small numbers and the ambiguity can be resolved only by analytically continuing $R_{n_e}^{\eta=\infty}(y)$.

For $y \rightarrow 1$, the general prediction from CFT (74) for $c = 1$ is

$$\mathcal{E}(y) = -\frac{1}{4} \ln(1-y) + \dots, \quad (201)$$

however, we have shown in Eq. (106) that for the model at hand, subleading double logarithmic corrections are present

$$\mathcal{E}(y) = -\frac{1}{4} \ln(1-y) - \frac{1}{2} \ln K(y) - \ln P_1 + o(1), \quad (202)$$

where $K(y)$ is the elliptic integral of the first kind and $P_1 = 0.832056\dots$ is given in Eq. (114). Written in this form, the expansion contains also some of the subleading corrections (in $1-y$) and it is expected to describe the data better. Indeed in Fig. 12, this prediction is almost indistinguishable from the data all the way from $y \sim 1$ (where it is an exact result) down to $y \sim 0.3$. We should mention that the subleading logarithmic correction may be responsible for the exponent $1/3$ found in Ref. [12] as compared with our analytic result $1/4$.

Finally we would like to mention that, in a long enough chain, when each interval contains a *finite* number of lattice points, the negativity must vanish exactly for

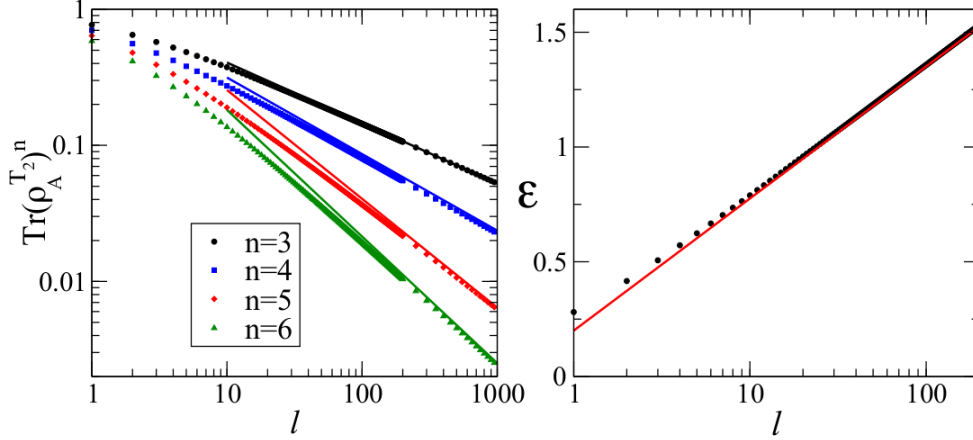


Figure 13. $\text{Tr}(\rho_A^{T_2})^n$ (left) and logarithmic negativity (right) for a semi-infinite critical ($\omega = 0$) harmonic chain with Dirichlet boundary conditions in the origin. We report the results for two adjacent intervals of equal length l with the first one starting from the origin. The data are perfectly described by the asymptotic CFT predictions reported as solid lines.

sufficiently large separations. Indeed the reduced density matrix ρ_A has all strictly positive eigenvalues and in the limit when the intervals are far apart ρ_A factorizes and each factor is a finite matrix with positive eigenvalues which become independent of the separation. Thus, when we take the partial transpose, the change in the density matrix, and therefore in the eigenvalues, can be made arbitrarily small since $\langle p_i p_j \rangle$ (which is the correlator that changes sign, cf. Eq. (190)) decreases like $|i - j|^{-2}$. Thus the partial transpose changes the elements of ρ_A but an amount which is arbitrarily small so the eigenvalues do not change sign. Indeed this is consistent with the well-known result [1, 9] that the entanglement of two far away sites is exactly zero.

7.7. Tripartite chains with Dirichlet boundary in the origin

Now we consider the non-trivial case of a tripartite chain on a system with boundaries discussed in Sec. 6, which is the semi-infinite line, with $A_1 = [0, \ell]$, $A_2 = [\ell, 2\ell]$ and B the remainder. In this case, the results for $\text{Tr}(\rho_A^{T_2})^n$ are given in Eq. (166) which we report also here:

$$\text{Tr}(\rho_A^{T_2})^n = \begin{cases} \ell^{-c/6(n-1/n)} & n \text{ odd,} \\ \ell^{-c/12(n-1/n)-c/6(n/2-2/n)} & n \text{ even.} \end{cases} \quad (203)$$

The most interesting feature is the peculiar behavior for n even, which can be explicitly checked by considering the semi-infinite harmonic chain with $\omega = 0$. The results for the numerical evaluation of $\text{Tr}(\rho_A^{T_2})^n$ are reported in Fig. 13 (left), showing the perfect agreement of both even and odd $n = 3, 4, 5, 6$ where only the global amplitude has been fixed with a fit. The right panel of the same figure shows the corresponding logarithmic negativity which turns out to be described by the CFT prediction $\mathcal{E} = 1/4 \ln \ell + \text{const.}$

8. Some scaling considerations for massive theories

It is well known that for a gapped one-dimensional model, increasing ℓ the entanglement (Rényi) entropy saturates to a finite value [30]. The calculation of this saturation value is generically complicated because it depends on microscopical details of the model and so it is calculable only for few simple integrable cases (see e.g. [22, 69, 70]). However, some general results can be worked out when a system is close to a conformal quantum critical point, and in the scaling limit where the lattice spacing $a \rightarrow 0$ and with the correlation length fixed and large. Under these hypotheses and when all the lengths of the various subsystems (and so the total one for a finite system) are much larger than ξ which is itself large, the Rényi entropies are [22]

$$S_A^{(n)} = \mathcal{A} \frac{c}{12} \left(1 + \frac{1}{n}\right) \log \frac{\xi}{a} + O(\xi^0), \quad (204)$$

where \mathcal{A} is the number of boundary points between A and its complement and c is the central charge of the conformal field theory for $\xi^{-1} = 0$. Clearly, when the interval lengths are of the order of ξ , a complicated and universal (within the scaling limit) crossover takes place, which has been worked out only in very few QFT [22, 24, 71, 72].

The same difficulties for the entanglement entropy, with also some additional problems, make prohibitive the calculations of the negativity and $\text{Tr}(\rho_A^{T_2})^n$ for a general gapped model. However, in the scaling limit and when the correlation length is itself large, but smaller than all the subsystems lengths, scaling considerations lead to very general results. For example in the case of a bipartition of a pure state in a finite interval of length $\ell \gg \xi$ and the remainder, the scaling suggests to replace ℓ with ξ in Eqs. (42) and (43) for $\text{Tr}(\rho_A^{T_2})^n$ and so the negativity is

$$\mathcal{E} = \frac{c}{2} \ln \xi + O(\xi^0). \quad (205)$$

This is clearly true because it is the general relation (21) between negativity and Rényi entropy. A direct check of this is the general result for a bisected harmonic chain (i.e. A_2 formed by $N/2$ consecutive sites and A_1 the remainder) with periodic boundary conditions and nearest neighbor interaction. In this case, an interesting exact formula has been found for the logarithmic negativity [10]

$$\mathcal{E} = \frac{1}{4} \ln \left(1 + \frac{4K}{M\omega^2}\right), \quad (206)$$

which, remarkably, is independent of the size of the chain N . In the limit $\xi^{-1} \propto \omega \ll 1$ gives $\mathcal{E} = (\ln \xi)/2$, in agreement with the general scaling.

A more interesting example can be obtained by considering the case of two adjacent intervals. Again, scaling suggests to substitute in Eq. (50) for the conformal case $\ell_{1,2}$ with ξ giving

$$\mathcal{E} = \frac{c}{4} \ln \xi + O(\xi^0). \quad (207)$$

This scaling in ξ is checked in Fig. 14 (left) for the harmonic chain for two adjacent intervals of the same length ℓ . This shows an excellent agreement for $1 \ll \xi \ll \ell$ while for larger ξ , the crossover to the CFT prediction (50) takes place.

On the same lines as above, the negativity for other tripartitions can be deduced by means of simple scaling arguments.

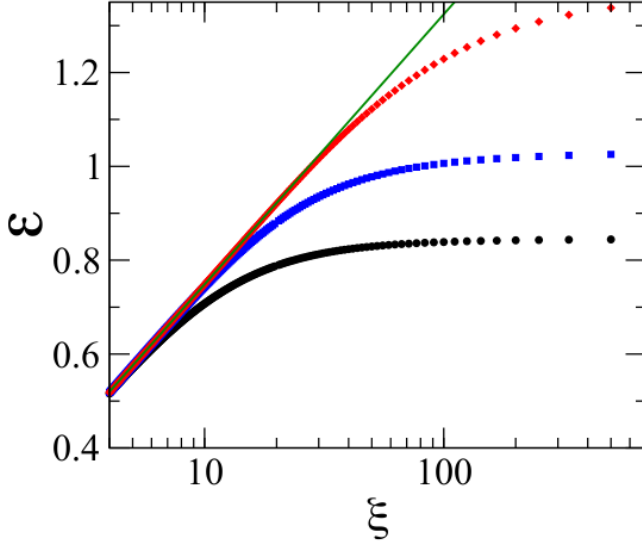


Figure 14. The negativity \mathcal{E} for two adjacent intervals of length $\ell = 10, 20, 50$ (from bottom to top) in a periodic system of total length $L = 150$. For $\xi \leq \ell$ all data collapse on the scaling prediction (207) while, when ξ becomes of order ℓ , a crossover to the CFT scaling form takes place.

9. Conclusions

We introduced a general field theoretical formalism to calculate the negativity and the logarithmic negativity, as an extension of our previous short communication [21]. This novel approach is based on a replica calculation of the traces of even integers n_e powers of the partial transpose of the reduced density matrix and analytically continuing this to $n_e \rightarrow 1$, i.e. the logarithmic negativity is

$$\mathcal{E} = \lim_{n_e \rightarrow 1} \ln \text{Tr}(\rho_A^{T_2})^{n_e}. \quad (208)$$

Several physical situations have been explicitly worked out for a conformally invariant theory:

- The case in which A_1 is an interval and A_2 the remainder of an infinite, semi-infinite or finite (both periodic and with boundaries) system.
- The case in which A_1 and A_2 are two adjacent intervals of length ℓ_1 and ℓ_2 respectively. For an infinite system the negativity is

$$\mathcal{E} = \frac{c}{4} \ln \frac{\ell_1 \ell_2}{\ell_1 + \ell_2} + \text{cnst}. \quad (209)$$

This is simply generalized to a finite periodic system.

- For the case in which A_1 and A_2 are two disjoint intervals (always of length ℓ_1 and ℓ_2), the negativity turns out to depend on the full operator content of the theory and it is a *scale invariant function* (i.e. a function of the harmonic ratio of the four points defining the two intervals). We calculated the traces of integer powers of the partial transposed reduced density matrix for a free bosonic theory, both compactified (i.e. the Luttinger liquid field theory) and in the limit

of infinite compactification radius. However, the n dependence of these formulas is too complicated and we managed to calculate the analytic continuation only in some physical relevant limits (far and close intervals).

All the CFT results have been accurately checked for a chain of harmonic oscillators, finding perfect agreement. We also proposed a few scaling relations valid in the scaling regime when a theory is close to a conformal quantum critical point, and the correlation length (inverse gap or mass) is finite but large.

We are currently working out the generalization of the CFT approach to finite temperature field theories which is not as straightforward as it could naively appear. Finally, we mention that it is of extreme interest to check numerically all our CFT predictions in more complicated lattice models such as spin-chains and itinerant fermions described by the Luttinger liquid field theory, for which we worked out explicit predictions for $\text{Tr}(\rho_A^{T_2})^n$ even in the case of disjoint intervals.

Acknowledgments

ET thanks Marcus Cramer for discussions. This work was supported by the ERC under Starting Grant 279391 EDEQS (PC). This work has been partly done when all the authors were guests of the Galileo Galilei Institute in Florence and Institut Henri Poincaré in Paris. ET thanks the Dipartimento di Fisica dell'Università di Pisa for the warm hospitality during the last part of this work.

References

- [1] L. Amico, R. Fazio, A. Osterloh, and V. Vedral, Entanglement in many-body systems, *Rev. Mod. Phys.* **80**, 517 (2008); J. Eisert, M. Cramer, and M. B. Plenio, Area laws for the entanglement entropy - a review, *Rev. Mod. Phys.* **82**, 277 (2010); Entanglement entropy in extended systems, P. Calabrese, J. Cardy, and B. Doyon Eds, *J. Phys. A* **42** 500301 (2009).
- [2] G. Vidal, Entanglement monotones, *J. Mod. Opt.* **47** (2000) 355.
- [3] P. Calabrese and A. Lefevre, Entanglement spectrum in one-dimensional systems, *Phys. Rev. A* **78**, 032329 (2008).
- [4] M. B. Plenio and S. Virmani, An introduction to entanglement measures, *Quant. Inf. Comput.* **7**, 1 (2007).
- [5] F. Verstraete, J. J. Garcia-Ripoll, and J. I. Cirac, Matrix Product Density Operators: Simulation of finite-T and dissipative systems, *Phys. Rev. Lett.* **93**, 207204 (2004); M. Zwolak and G. Vidal, Mixed-state dynamics in one-dimensional quantum lattice systems: a time-dependent superoperator renormalization algorithm, *Phys. Rev. Lett.* **93**, 207205 (2004).
- [6] J. Eisert and M. B. Plenio, A Comparison of entanglement measures, *J. Mod. Opt.* **46**, 145 (1999).
- [7] A. Peres, Separability criterion for density matrices, *Phys. Rev. Lett.* **77**, 1413 (1996); M. Horodecki, P. Horodecki and R. Horodecki, Mixed state entanglement and distillation: Is there a 'bound' entanglement in nature?, *Phys. Rev. Lett.* **80**, 5239 (1998); K. Zyczkowski, P. Horodecki, A. Sanpera and M. Lewenstein, On the volume of the set of mixed entangled states, *Phys. Rev. A* **58**, 883 (1998); L. M. Duan, G. Giedke, J. I. Cirac and P. Zoller, Inseparability criterion for continuous variables systems *Phys. Rev. Lett.* **84**, 2722 (2000); R. Simon, Peres-Horodecki separability criterion for continuous variables systems *Phys. Rev. Lett.* **84**, 2726 (2000).
- [8] G. Vidal and R. F. Werner, A computable measure of entanglement, *Phys. Rev. A* **65**, 032314 (2002).
- [9] A. Osterloh, L. Amico, G. Falci, and R. Fazio, Scaling Properties of the Entanglement at a Quantum Phase Transition, *Nature* **416**, 608 (2002).
- [10] K. Audenaert, J. Eisert, M. B. Plenio and R. F. Werner, Entanglement Properties of the Harmonic Chain, *Phys. Rev. A* **66**, 042327 (2002).
- [11] H. Wichterich, J. Molina-Vilaplana, and S. Bose, Scale invariant entanglement at quantum phase transitions, *Phys. Rev. A* **80**, 010304 (2009).

- [12] S. Marcovitch, A. Retzker, M. B. Plenio, and B. Reznik, Critical and noncritical long range entanglement in the Klein-Gordon field, *Phys. Rev. A* **80**, 012325 (2009).
- [13] H. Wichterich, J. Vidal, and S. Bose, Universality of the negativity in the Lipkin-Meshkov-Glick model, *Phys. Rev. A* **81**, 032311 (2010).
- [14] A. Bayat, P. Sodano, and S. Bose, Negativity as the Entanglement Measure to Probe the Kondo Regime in the Spin-Chain Kondo Model, *Phys. Rev. B* **81**, 064429 (2010).
- [15] A. Bayat, S. Bose, P. Sodano, and H. Johannesson, Entanglement probe of two-impurity Kondo physics in a spin chain, *Phys. Rev. Lett.* **109**, 066403 (2012).
- [16] A. Bayat, P. Sodano, and S. Bose, Entanglement Routers Using Macroscopic Singlets, *Phys. Rev. Lett.* **105**, 187204 (2010).
- [17] P. Sodano, A. Bayat, and S. Bose Kondo Cloud Mediated Long Range Entanglement After Local Quench in a Spin Chain, *Phys. Rev. B* **81**, 100412 (2010).
- [18] J. Anders and A. Winter, Entanglement and separability of quantum harmonic oscillator systems at finite temperature *Quant. Inf. Comput.* **8**, 245 (2008).
- [19] J. Anders, Thermal state entanglement in harmonic lattices, *Phys. Rev. A* **77**, 062102 (2008).
- [20] A. Ferraro, D. Cavalcanti, A. Garcia-Saez, and A. Acin, Thermal bound entanglement in macroscopic systems and area laws, *Phys. Rev. Lett.* **100**, 080502 (2008).
- [21] P. Calabrese, J. Cardy, and E. Tonni, Entanglement negativity and quantum field theory, *Phys. Rev. Lett.* **109**, 130502 (2012).
- [22] P. Calabrese and J. Cardy, Entanglement entropy and quantum field theory, *J. Stat. Mech.* P06002 (2004).
- [23] P. Calabrese and J. Cardy, Entanglement entropy and conformal field theory, *J. Phys. A* **42**, 504005 (2009).
- [24] J. L. Cardy, O.A. Castro-Alvaredo, and B. Doyon, Form factors of branch-point twist fields in quantum integrable models and entanglement entropy, *J. Stats. Phys.* **130** (2008) 129.
- [25] F. Gliozzi and L. Tagliacozzo, Entanglement entropy and the complex plane of replicas, *J. Stat. Mech.* P01002 (2010).
- [26] J. Kurchan, Replica trick to calculate means of absolute values: applications to stochastic equations, *J. Phys. A* **24**, 4969 (1991).
- [27] D. M. Gangardt and A. Kamenev, Replica Treatment of the Calogero-Sutherland Model, *Nucl. Phys. B* **610**, 578 (2001); S. M. Nishigaki, D. M. Gangardt, and A. Kamenev, Correlation functions of the BC Calogero-Sutherland model, *J. Phys. A* **36**, 3137 (2003); D. M. Gangardt, Universal correlations of trapped one-dimensional impenetrable bosons, *J. Phys. A* **37**, 9335 (2004); D. M. Gangardt and G. V. Shlyapnikov, Off-diagonal correlations of lattice impenetrable bosons in one dimension, *New J. of Phys.* **8**, 167 (2006); P. Calabrese and R. Santachiara, Off-diagonal correlations in one-dimensional anyonic models: A replica approach, *J. Stat. Mech.* P03002 (2009).
- [28] M. Bianchi, G. Pradisi, and A. Sagnotti, Toroidal compactification and symmetry breaking in open string theories, *Nucl. Phys. B* **376**, 365 (1992); see also chapter 6.4 of R. Blumenhagen and E. Plauschinn, *Introduction to conformal field theory with application to string theory*, Springer (2009).
- [29] C. Holzhey, F. Larsen, and F. Wilczek, Geometric and renormalized entropy in conformal field theory, *Nucl. Phys. B* **424**, 443 (1994); C. G. Callan and F. Wilczek, On geometric entropy. *Phys. Lett. B* **333**, 55 (1994).
- [30] G. Vidal, J. I. Latorre, E. Rico, and A. Kitaev, Entanglement in quantum critical phenomena, *Phys. Rev. Lett.* **90**, 227902 (2003); J. I. Latorre, E. Rico, and G. Vidal, Ground state entanglement in quantum spin chains, *Quant. Inf. Comp.* **4**, 048 (2004).
- [31] M. Fagotti, P. Calabrese, and J. E. Moore, Entanglement spectrum of random-singlet quantum critical points, *Phys. Rev. B* **83**, 045110 (2011).
- [32] I. Affleck and A. W. W. Ludwig, Universal non-integer “ground-state degeneracy” in critical quantum systems, *Phys. Rev. Lett.* **67**, 161 (1991).
- [33] H.-Q. Zhou, T. Barthel, J. O. Fjaerestad, and U. Schollwoeck, Entanglement and boundary critical phenomena, *Phys. Rev. A* **74**, 050305 (2006).
- [34] P. Calabrese, J. Cardy, and E. Tonni, Entanglement entropy of two disjoint intervals in conformal field theory, *J. Stat. Mech.* P11001 (2009).
- [35] P. Calabrese, J. Cardy, and E. Tonni, Entanglement entropy of two disjoint intervals in conformal field theory II, *J. Stat. Mech.* P01021 (2011).
- [36] S. Furukawa, V. Pasquier, and J. Shiraishi, Mutual information and compactification radius in a $c=1$ critical phase in one dimension, *Phys. Rev. Lett.* **102**, 170602 (2009).
- [37] M. Caraglio and F. Gliozzi, Entanglement entropy and twist fields, *JHEP* 0811: 076 (2008).
- [38] H. Casini, C. D. Fosco, and M. Huerta, Entanglement and alpha entropies for a massive Dirac

- field in two dimensions, *J. Stat. Mech.* P05007 (2005); H. Casini and M. Huerta, Remarks on the entanglement entropy for disconnected regions, *JHEP* 0903: 048 (2009); H. Casini and M. Huerta, Reduced density matrix and internal dynamics for multicomponent regions, *Class. Quant. Grav.* **26**, 185005 (2009); H. Casini, Entropy inequalities from reflection positivity, *J. Stat. Mech.* (2010) P08019.
- [39] P. Facchi, G. Florio, C. Invernizzi, and S. Pascazio, Entanglement of two blocks of spins in the critical Ising model, *Phys. Rev. A* **78**, 052302 (2008).
 - [40] I. Klich and L. Levitov, Quantum noise as an entanglement meter, *Phys. Rev. Lett.* **102**, 100502 (2009).
 - [41] V. Alba, L. Tagliacozzo, and P. Calabrese, Entanglement entropy of two disjoint blocks in critical Ising models, *Phys. Rev. B* **81** 060411 (2010).
 - [42] V. Alba, L. Tagliacozzo, and P. Calabrese, Entanglement entropy of two disjoint intervals in $c = 1$ theories, *J. Stat. Mech.* (2011) P06012.
 - [43] M. Fagotti and P. Calabrese, Entanglement entropy of two disjoint blocks in XY chains, *J. Stat. Mech.* (2010) P04016.
 - [44] P. Calabrese, Entanglement entropy in conformal field theory: New results for disconnected regions, *J. Stat. Mech.* (2010) P09013.
 - [45] F. Igloi and I. Peschel, On reduced density matrices for disjoint subsystems, 2010 *EPL* **89** 40001.
 - [46] M. Headrick, Entanglement Renyi entropies in holographic theories, *Phys. Rev. D* **82**, 126010 (2010).
 - [47] M. Fagotti, New insights into the entanglement of disjoint blocks, *EPL* **97**, 17007 (2012).
 - [48] M. A. Rajabpour and F. Gliozzi, Entanglement entropy of two disjoint intervals from fusion algebra of twist fields, *J. Stat. Mech.* (2012) P02016.
 - [49] B. Swingle, Rényi entropy, mutual information, and fluctuation properties of Fermi liquids, *Phys. Rev. B* **86**, 045109 (2012); P. Calabrese, M. Mintchev, and E. Vicari, Exact relations between particle fluctuations and entanglement in Fermi gases, *EPL* **98**, 20003 (2012).
 - [50] J. Molina-Vilaplana and P. Sodano, Holographic View on Quantum Correlations and Mutual Information between Disjoint Blocks of a Quantum Critical System, *JHEP* 10 (2011) 011.
 - [51] S. Ryu and T. Takayanagi, Holographic derivation of entanglement entropy from AdS/CFT, *Phys. Rev. Lett.* **96** (2006) 181602; S. Ryu and T. Takayanagi, Aspects of holographic entanglement entropy, *JHEP* 0608: 045 (2006); V. E. Hubeny and M. Rangamani, Holographic entanglement entropy for disconnected regions, *JHEP* 0803: 006 (2008); M. Headrick and T. Takayanagi, A holographic proof of the strong subadditivity of entanglement entropy, *Phys. Rev. D* **76**, 106013 (2007); T. Nishioka, S. Ryu, and T. Takayanagi, Holographic entanglement entropy: an overview, *J. Phys. A* **42** (2009) 504008; E. Tonni, Holographic entanglement entropy: near horizon geometry and disconnected regions, *JHEP* 1105:004 (2011).
 - [52] M. Headrick, A. Lawrence, and M. M. Roberts, Bose-Fermi duality and entanglement entropies, *arXiv:1209.2428*.
 - [53] A. Erdelyi, Higher transcendental functions, Mc Graw Hill, (1953).
 - [54] L. J. Dixon, D. Friedan, E. J. Martinec and S. H. Shenker, The Conformal Field Theory of Orbifolds, *Nucl. Phys. B* **282** (1987) 13.
 - [55] A. B. Zamolodchikov, Conformal scalar field on the hyperelliptic curve and critical Ashkin-Teller multipoint correlation functions, *Nucl. Phys. B* **285** (1987) 481.
 - [56] R. Dijkgraaf, E. P. Verlinde and H. L. Verlinde, $C = 1$ Conformal Field Theories on Riemann Surfaces, *Commun. Math. Phys.* **115** (1988) 649.
 - [57] I. Peschel and M.-C. Chung, Density Matrices for a Chain of Oscillators, *J. Phys. A* **32**, 8419 (1999); I. Peschel and V. Eisler, Exact results for the entanglement across defects in critical chains, *J. Phys. A* **45** (2012) 155301.
 - [58] I. Peschel, Calculation of reduced density matrices from correlation functions *J. Phys. A* **36**, L205 (2003).
 - [59] A. Botero and B. Reznik, Spatial structures and localization of vacuum entanglement in the linear harmonic chain, *Phys. Rev. A* **70**, 052329 (2004).
 - [60] M. B. Plenio, J. Eisert, J. Dreissig, and M. Cramer, Entropy, entanglement, and area: analytical results for harmonic lattice systems, *Phys. Rev. Lett.* **94**, 060503 (2005); M. Cramer, J. Eisert, M. B. Plenio, and J. Dreissig An entanglement-area law for general bosonic harmonic lattice systems *Phys. Rev. A* **73** (2006) 012309.
 - [61] I. Peschel and V. Eisler, Reduced density matrices and entanglement entropy in free lattice models, *J. Phys. A* **42**, 504003 (2009).
 - [62] S. Lievens, N. I. Stoilova and J. Van der Jeugt, Harmonic oscillator chains as Wigner Quantum Systems: Periodic and fixed wall boundary conditions in $gl(1 - n)$ solutions, *J. Math. Phys.* **49** (2008) 073502.

- [63] P. Di Francesco, P. Mathieu, and D. Senechal, *Conformal Field Theory* (Springer-Verlag, New York, 1997).
- [64] P. Calabrese, M. Campostrini, F. Essler, and B. Nienhuis, Parity effects in the scaling of block entanglement in gapless spin chains, *Phys. Rev. Lett.* **104**, 095701 (2010).
- [65] J. Cardy and P. Calabrese, Unusual corrections to scaling in entanglement entropy, *J. Stat. Mech.* (2010) P04023.
- [66] P. Calabrese and F. H. L. Essler, Universal corrections to scaling for block entanglement in spin-1/2 XX chains, *J. Stat. Mech.* (2010) P08029.
- [67] J. L. Cardy, Conformal invariance and surface critical behaviour, *Nucl. Phys. B* **240**, 514 (1984).
- [68] M. Fagotti and P. Calabrese, Universal parity effects in the entanglement entropy of XX chains with open boundary conditions, *J. Stat. Mech.* P01017 (2011).
- [69] A. R. Its, B.-Q. Jin, and V. E. Korepin, Entanglement in XY spin chain, *J. Phys. A* **38**, 2975 (2005); F. Franchini, A. R. Its, and V. E. Korepin, Renyi entropy of the XY spin chain, *J. Phys. A* **41**, 025302 (2008).
- [70] I. Peschel, On the entanglement entropy for a XY spin chain, *J. Stat. Mech.* (2004) P12005; R. Weston, The Entanglement Entropy of Solvable Lattice Models, *J. Stat. Mech.* L03002 (2006); P. Calabrese, J. Cardy, and I. Peschel, Corrections to scaling for block entanglement in massive spin-chains, *J. Stat. Mech.* P09003 (2010); E. Ercolessi, S. Evangelisti, and F. Ravanini, Exact entanglement entropy of the XYZ model and its sine-Gordon limit, *Phys. Lett. A* **374**, 2101 (2010).
- [71] H. Casini and M. Huerta, Entanglement entropy in free quantum field theory, *J. Phys. A* **42**, 504007 (2009); H. Casini and M. Huerta, Analytic results on the geometric entropy for free fields, *J. Stat. Mech.* P01012 (2008); H. Casini and M. Huerta Entanglement and alpha entropies for a massive scalar field in two dimensions, *J. Stat. Mech.* P12012 (2005).
- [72] O. A. Castro-Alvaredo and B. Doyon, Bipartite entanglement entropy in massive 1+1-dimensional quantum field theories, *J. Phys. A* **42** 504006 (2009); O. A. Castro-Alvaredo and B. Doyon, Bipartite entanglement entropy in massive QFT with a boundary: the Ising model *J. Stat. Phys.* **134**, 105 (2009); B. Doyon, Bipartite entanglement entropy in massive two-dimensional quantum field theory, *Phys. Rev. Lett.* **102**, 031602 (2009); O. A. Castro-Alvaredo and B. Doyon, Bipartite entanglement entropy in integrable models with backscattering, *J. Phys. A* **41** 275203 (2008).